

Search for Transcriptional and Metabolic Markers of Grape Pre-Ripening and Ripening and Insights into Specific Aroma Development in Three Portuguese Cultivars

Patricia Agudelo-Romero¹✉, Alexander Erban²✉, Lisete Sousa³, Maria Salomé Pais¹, Joachim Kopka², Ana Margarida Fortes¹*

1 Universidade de Lisboa, Faculdade de Ciências de Lisboa, Center for Biodiversity, Functional & Integrative Genomics, Campo Grande, Lisboa, Portugal, **2** Max-Planck-Institut für Molekulare Pflanzenphysiologie, Potsdam, Golm, Germany, **3** Department of Statistics and Operational Research, Centro de Estatística e Aplicações da UL, Faculdade de Ciências de Lisboa, Lisbon, Portugal

Abstract

Background: Grapes (*Vitis* species) are economically the most important fruit crop worldwide. However, the complexity of molecular and biochemical events that lead to ripening of berries as well as how aroma is developed are not fully understood.

Methodology/Principal Findings: In an attempt to identify the common mechanisms associated with the onset of ripening independently of the cultivar, grapes of Portuguese elite cultivars, Trincadeira, Aragonês, and Touriga Nacional, were studied. The mRNA expression profiles corresponding to *veraison* (EL35) and mature berries (EL36) were compared. Across the three varieties, 9,8% (2255) probesets corresponding to 1915 unigenes were robustly differentially expressed at EL 36 compared to EL 35. Eleven functional categories were represented in this differential gene set. Information on gene expression related to primary and secondary metabolism was verified by RT-qPCR analysis of selected candidate genes at four developmental stages (EL32, EL35, EL36 and EL 38). Gene expression data were integrated with metabolic profiling data from GC-EI-TOF/MS and headspace GC-EI-MS platforms.

Conclusions/Significance: Putative molecular and metabolic markers of grape pre-ripening and ripening related to primary and secondary metabolism were established and revealed a substantial developmental reprogramming of cellular metabolism. Altogether the results provide valuable new information on the main metabolic events leading to grape ripening. Furthermore, we provide first hints about how the development of a cultivar specific aroma is controlled at transcriptional level.

Citation: Agudelo-Romero P, Erban A, Sousa L, Pais MS, Kopka J, et al. (2013) Search for Transcriptional and Metabolic Markers of Grape Pre-Ripening and Ripening and Insights into Specific Aroma Development in Three Portuguese Cultivars. PLoS ONE 8(4): e60422. doi:10.1371/journal.pone.0060422

Editor: Miguel A. Blazquez, Instituto de Biología Molecular y Celular de Plantas, Spain

Received: January 10, 2013; **Accepted:** February 25, 2013; **Published:** April 2, 2013

Copyright: © 2013 Agudelo-Romero et al. This is an open-access article distributed under the terms of the Creative Commons Attribution License, which permits unrestricted use, distribution, and reproduction in any medium, provided the original author and source are credited.

Funding: Funding was provided by the Portuguese Foundation for Science and Technology (FCT) through a Post-doctoral fellowship to Patricia Agudelo-Romero (SFRH/BPD/72070/2010) and Auxiliar Researcher contract Ciência 2008 to Ana M. Fortes (C2008-UL-BioFIG-5). Additional funding was provided by the FCT project PTDC/AGR-GPL/100919/2008, and ERA-PG (FCT ERA-PG/0004/2006) under the project Genomic Research-Assisted breeding for Sustainable Production of Quality GRAPES and WINE (<http://urgi.versailles.inra.fr/projects/GRASP/>). This work was developed within the BioFig Center with reference PEst-OE/BIA/UI4046/2011 with participation of CEAUL (PEst-OE/MAT/UI0006/2011). The funders had no role in study design, data collection and analysis, decision to publish, or preparation of the manuscript.

Competing Interests: The authors have declared that no competing interests exist.

* E-mail: amfortes@fc.ul.pt

✉ These authors contributed equally to this work.

Introduction

Grapes (*Vitis* species) are economically the most important fruit crop worldwide due to their use in production of wine, grape juice, table grapes, among other. The consumption of grapes and wine presents numerous nutritional and health benefits for humans [1]. Grape seeds have significant content of phenolic compounds such as gallic acid, catechin and epicatechin, and a wide variety of proanthocyanidins which demonstrate significant cancer prevention potential [2]. Red wines contain more than 200 polyphenolic compounds that are thought to act as antioxidants. In particular,

resveratrol exhibits cardioprotective effects and anticancer properties [2].

The Vitaceae family consists of approximately one thousand species grouped in seventeen genera. The most cultivated *Vitis vinifera* comprises up to 5000 true cultivars. In traditional vine areas, the production should present typicity that is dependent on grapevine variety among other factors. Therefore, vine improvement, specifically the regional development of typical wines, is greatly limited to the natural variability of available cultivars. In this respect, the less known Portuguese and Spanish cultivars offer plenty of choice to develop wines with different characteristics that

may constitute a competitive advantage in a demanding global market.

The Portuguese wines are traditionally made by blending generally three or four varieties. Nevertheless, following a recent consumer trend the cultivars Touriga Nacional, Trincadeira and Aragonês have been used to produce high quality monovarietal red wines. Their exceptional characteristics such as the potential to produce highly aromatic wines have recently attracted the interest of vine growers and viticulturists abroad with the aim of introducing new competitive products into the market. Touriga Nacional is considered to be one of the most, if not the most important native variety in Portugal despite its tiny berries with a high skin to pulp ratio. Aragonês, also called Tinta Roriz in Northern Portugal or Tempranillo in Spain, offers high yields and is indispensable in the blend of a good Porto wine. Trincadeira is ideally suited to grow in hot, dry and very bright areas, but has varying (irregular) yield and is prone to infection with pathogenic moulds. However, in good years Trincadeira will produce exceptionally great wines.

The process of development and ripening of non-climacteric fruits such as grapes is not well known. Grape berry development consists of two successive sigmoidal growth periods separated by a lag phase; from anthesis to ripening grape development can be divided into three major phases [3] with more detailed descriptive designations, known as the modified E-L system, being used to define more precise growth stages over the entire grapevine lifecycle [4]. During the first growth period, the berry is formed, and biosynthesis of tannins and hydroxycinnamic acids occurs, as well as accumulation of organic acids, such as tartrate and malate. The onset of ripening, *véraison*, constitutes a transition phase during which growth declines and during which berries soften and color production is initiated, e.g. the anthocyanin accumulation in red grapes. Ripening, the final phase of cell expansion growth, is characterized by an increase in pH and accumulation of soluble sugars, anthocyanins and flavour-enhancing compounds.

Specific combinations of aromas, flavours, tannins, sugars and acids, create the unique “varietal character” of a ripe wine grape. The many chemical compounds contributing to flavour, i.e. the combination of taste and aroma, in wines are determined in the vineyard by interacting factors, such as the natural environment, vineyard management practices, and vine genotypes. Increased knowledge of the grape ripening process will contribute to maintain a sustainable production of high quality grapes in a changing environment, one major challenge for the viticulture in this century.

Recent reports characterized grape ripening of specific varieties, namely Shiraz [5], Cabernet Sauvignon [6], Pinot Noir [7], Barbera [8], Corvina [9], Muscat Hamburg [10] and Trincadeira [11]. More recently, a comparison was conducted between Cabernet Sauvignon and Norton grapes [12] regarding transcriptional regulation and flavonoid biosynthesis. These publications showed that activities of several metabolic pathways, including the tricarboxylic acid cycle, the shikimate pathway, and amino acid metabolism, shifted during fruit growth and ripening. Nevertheless, it is still difficult to ascertain which molecular and metabolic mechanisms are specific characteristics of a single variety and which can be considered general markers of ripening. It is particularly important to determine, how the nutritional quality for wine production purposes is achieved. In a previous NMR based study the quality of Trincadeira was associated with low phenolics content but higher sugars and organic acid levels while Touriga Nacional and Aragonês were characterized by high contents of phenolics and specific amino acids [13]. This NMR

analysis enabled the identification of approximately thirty metabolites.

We now report the GC-MS based metabolome analysis of the same cultivars that complements previous results and importantly increased the coverage to a total of 121 volatile and soluble taste and aroma components. Furthermore, we integrated information from transcriptomic and from paired metabolomic analyses and now apply two essential functional genomics tools to characterize and to establish common mechanisms and candidate markers of grape ripening among the three most important Portuguese grapevine varieties. Next to the robust responses of all varieties we searched for the specific properties and, thus, gather insights into how a cultivar specific aroma is developed.

Results and Discussion

Phenotypic and metabolic characterization of grape berries

Grape berries were sampled at four developmental stages according to EL system [4] during 2008 growing season. The staging took into account the berry weight and the content of the main anthocyanins, organic acids and sugars (Figs 1, 2). The developmental stages investigated in this study were identified as EL 32 characterized by small hard green berries accumulating organic acids, EL 35 corresponding to *véraison*, EL 36 involving sugar and anthocyanin accumulation, and active growth due to cell enlargement and EL 38 corresponding to harvest time. The date of *véraison* was set at approximately 9 weeks post-flowering for each of the three varieties.

Metabolic profiling of grapes was carried out using a GC-EI-TOF/MS platform that enabled the relative quantification of several classes of compounds such as fatty acids, phenylpropanoids and sugars among the polar compounds (Table 1, File S1). Additional metabolic profiling was achieved using a headspace GC-EI-MS platform for the relative quantification of volatiles. In what concerns amino acids, few could be quantified since the conditions used favored the identification of secondary metabolites. Homoserine and pyroglutamic acid which includes glutamine and glutamic acid were the amino acids identified (Table 1).

Specific chromatogram ion peaks were selected for relative quantification (based on peak height) of certain metabolites during ripening as shown in Fig. 2.

Regarding berry weight corresponding to ripe and harvest stages, Aragonês tends to present bigger berries, followed by Trincadeira and then Touriga Nacional. This implies that berries of Touriga Nacional contain a higher amount of skin per berry which may be related to the increased content in anthocyanins observed for this variety (Fig.1). The higher weight observed in Aragonês berries may also be partially responsible for higher content in fructose and glucose (Fig. 2) since these compounds accumulate preferentially in the pulp.

To confirm if these and other metabolites were present in significantly different amounts during ripening Kruskal-Wallis and Wilcoxon Rank sum tests were performed using ion peak responses (File S2). For the multiple comparisons the Benjamini & Hochberg correction was the most adequate. These tests showed that the majority of the metabolites (77, 69%) exhibited a different content either comparing among developmental stages or among varieties.

These ion peak responses were also used for Multivariate Data Analysis using the unsupervised method of Independent Principal Component analysis (ICA). A good discrimination was obtained between pre- *véraison*/*véraison* and post-*véraison* stages for all the varieties and both analysis of volatiles and polar metabolites

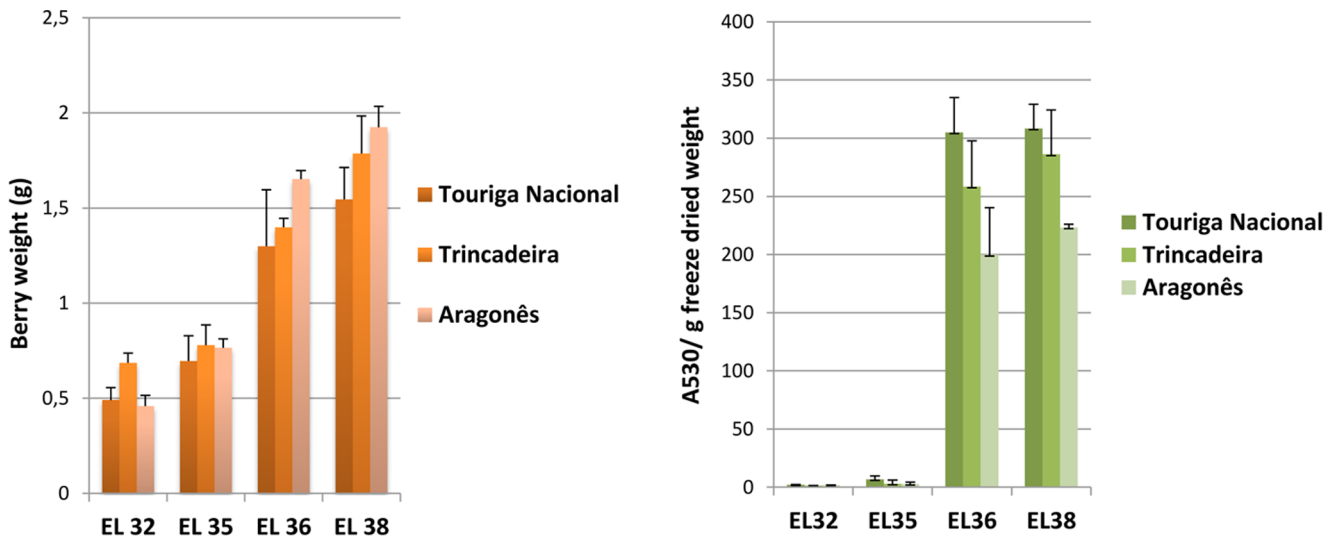


Figure 1. Fresh berry weight (g) and total anthocyanin content (absorbance at 530 nm per g of freeze dried material) of berries at developmental stages of EL 32, EL 35, EL 36 and EL 38. Bars represent standard deviation.
doi:10.1371/journal.pone.0060422.g001

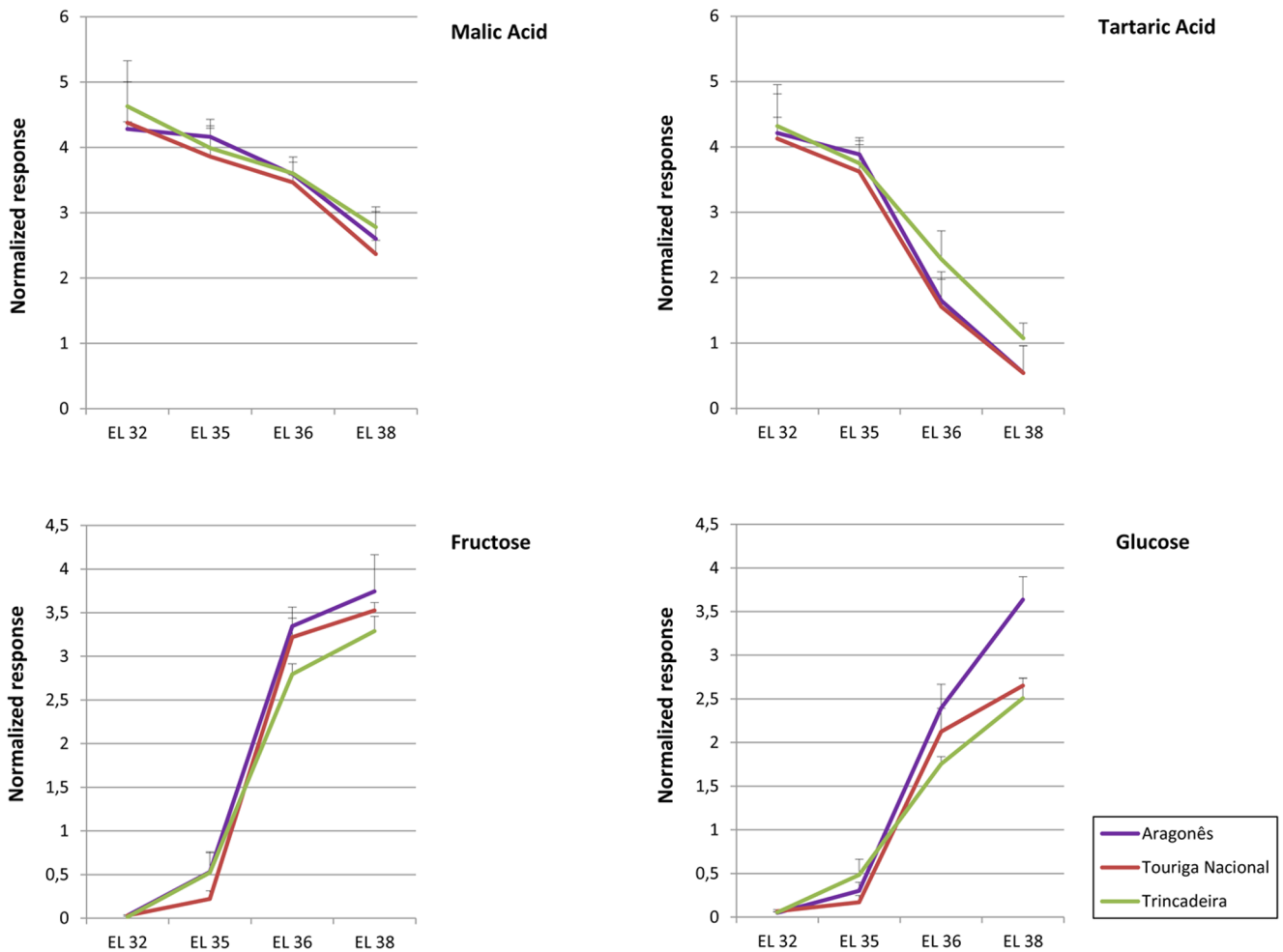


Figure 2. Relative quantification of malic acid, tartaric acid, fructose and glucose based on ion peak response. Malate and tartrate contents are higher at pre-*véraison* stages peaking at EL 32 whereas contents in fructose and glucose increase at post-*véraison* stages reaching maximal levels at EL 38.
doi:10.1371/journal.pone.0060422.g002

Table 1. List of metabolites identified by GC-EL-TOF/MS and GC-EL-MS during ripening of the three varieties.

Class	Metabolite
volatile	(E)-2-Heptenal
volatile	(E)-2-Hexenal
volatile	(E)-2-Pentenal
volatile	(E,E)-2,4-Hexadien-1-al
volatile	(Z)-3-Octen-1-ol
volatile	[3-Hydroxymandelic acid, ethyl ester, di-TMS]
volatile	2-Ethylfuran
volatile	2-Pentylfuran
volatile	3-Methylbutanal
volatile	3-Methylbutanol
volatile	6-Methyl-5-hepten-2-one
volatile	Benzaldehyde
volatile	Decanal
volatile	Ethanol
volatile	Hexanal
volatile	Nonanal
volatile	Octanal
volatile	Ethyl Acetate
volatile	Heptanal
volatile	Limonene
volatile	Undecane
acid	Aconitic acid, cis-
acid	Benzoic acid
acid	Benzoic acid, 3,4-dihydroxy-
acid	Butanoic acid, 2,4-dihydroxy-
acid	Citric acid
acid	Fumaric acid
acid	Gallic acid
acid	Gluconic acid, 2-oxo-
acid	Glutaric acid, 2-hydroxy-
acid	Glutaric acid, 2-oxo-
acid	Glutaric acid, 3-hydroxy-3-methyl-
acid	Glycolic acid
acid	Hexanoic acid, 2-ethyl-
acid	Lactic acid
acid	Malic acid
acid	Malic acid, 2-methyl-
acid	Pyruvic acid
acid	Shikimic acid
acid	Succinic acid
acid	Tartaric acid
acid	Vanillic acid
amino acid	Homoserine
amino acid	Pyroglutamic acid
fatty acid	Docosanoic acid
fatty acid	Eicosanoic acid
fatty acid	Hexacosanoic acid
fatty acid	Hexadecanoic acid
fatty acid	Hexanoic acid

Table 1. Cont.

Class	Metabolite
fatty acid	Nonanoic acid
fatty acid	Octacosanoic acid
fatty acid	Octadecadienoic acid, n-
fatty acid	Octadecanoic acid
fatty acid	Octadecen-1-ol, 9-(Z)-
fatty acid	Octadecenoic acid, 9-(Z)-
fatty acid	Tetracosanoic acid
fatty acid	Tetradecanoic acid
fatty acid	Triacontanoic acid
lipid	Ampelopsin
lipid	Campesterol
lipid	Phytol
lipid	Sitosterol, beta-
lipid	Stigmastan-3-ol, (3-beta)-
lipid	Tocopherol, alpha-
lipid	Tocopherol, beta-
N-compound	Ethanolamine
N-compound	Pyridine, 2-hydroxy-
N-compound	Pyridine, 3-hydroxy-
N-compound	Triethanolamine
phenylpropanoid	Quercetin
phenylpropanoid	Resveratrol, cis-
phenylpropanoid	Caffeic acid, trans-
phenylpropanoid	Catechin
phenylpropanoid	Epigallocatechin
phenylpropanoid	Cinnamic acid, 4-hydroxy-, trans-
phosphate	Ethanolaminephosphate
phosphate	Glycerol-3-phosphate
phosphate	Phosphoric acid
polyhydroxy acid	Dehydroascorbic acid dimer
polyhydroxy acid	Gluconic acid-1,5-lactone
polyhydroxy acid	Glyceric acid
polyhydroxy acid	Lyxonic acid
polyhydroxy acid	Threonic acid
polyhydroxy acid	Threonic acid-1,4-lactone
polyol	Erythritol
polyol	Glycerol
sugar	Fructose
sugar	Glucose
sugar	Sedoheptulose, 2,7-anhydro-, beta-
sugar	Sucrose

doi:10.1371/journal.pone.0060422.t001

(Fig. 3). However, the developmental stages of EL 32 and EL 35 (*véraison*) were only separated according to the polar metabolite fractions while samples corresponding to EL 36 and EL 38 clustered together in both types of analysis (though some degree of discrimination could be observed for polar metabolites). Regarding volatiles stages EL 35 and EL 32 were separated from EL 36 and EL 38 by two independent components accounting for 41.99% of variance. In what concerns polar metabolites the same

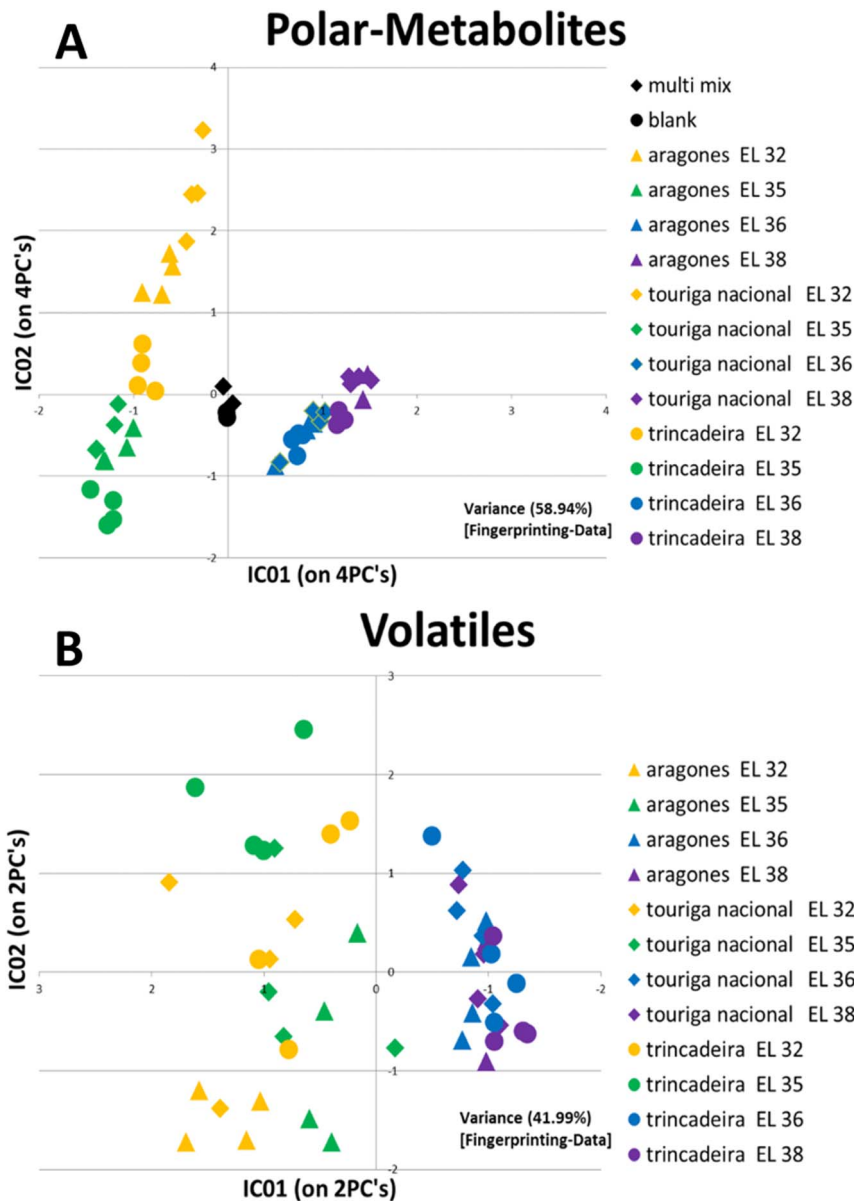


Figure 3. Score plot of ICA showing metabolic discrimination of developmental stages and cultivars. A Polar metabolites B Volatiles.
doi:10.1371/journal.pone.0060422.g003

discrimination accounted for 58.94% of variance. Trincadeira tends to cluster more independently of the other varieties as it has been previously observed using a NMR platform for metabolic profiling [13].

The heat map showed that the metabolites have a differential accumulation during berry development and ripening (Fig. 4). Some alcohols and aldehydes such as ethanol, (E)-2-hexenal and heptanal reached the highest levels in ripe and harvest stage of fruits, and contributed to the formation of aroma. The same holds true for sugars and many fatty acids. Organic acids tend to decrease during ripening in all varieties, though exhibiting a high degree of variance among them. Phosphoric acid was an exception since it increased at harvest stage in all varieties. Phenylpropanoids and flavonoids may also decrease or increase during ripening.

Microarray, functional categorization of Unigenes and RT-qPCR

The mRNA expression profiles of two time points (EL35 and EL36) during 2008 season were compared using the Affymetrix GrapeGen® genome array containing 23096 probesets corresponding to 18711 unique sequences. Testing was performed using biological triplicates for each time point. After performing a Bayes t-statistics from the linear models for microarray data (limma) for differential expression analysis, P-values were corrected for multiple-testing using the Benjamini-Hochberg's method [14]. The total number of probesets that were differentially expressed at least in one variety (fold change ≥ 1.5 and FDR < 0.05 or fold change ≤ -1.5 and FDR < 0.05) was 8696 corresponding to 37.65% of the total probesets represented in the chip (File S3). From these, a common gene set of 2255 probesets were differentially expressed in all the three studied varieties, whereas

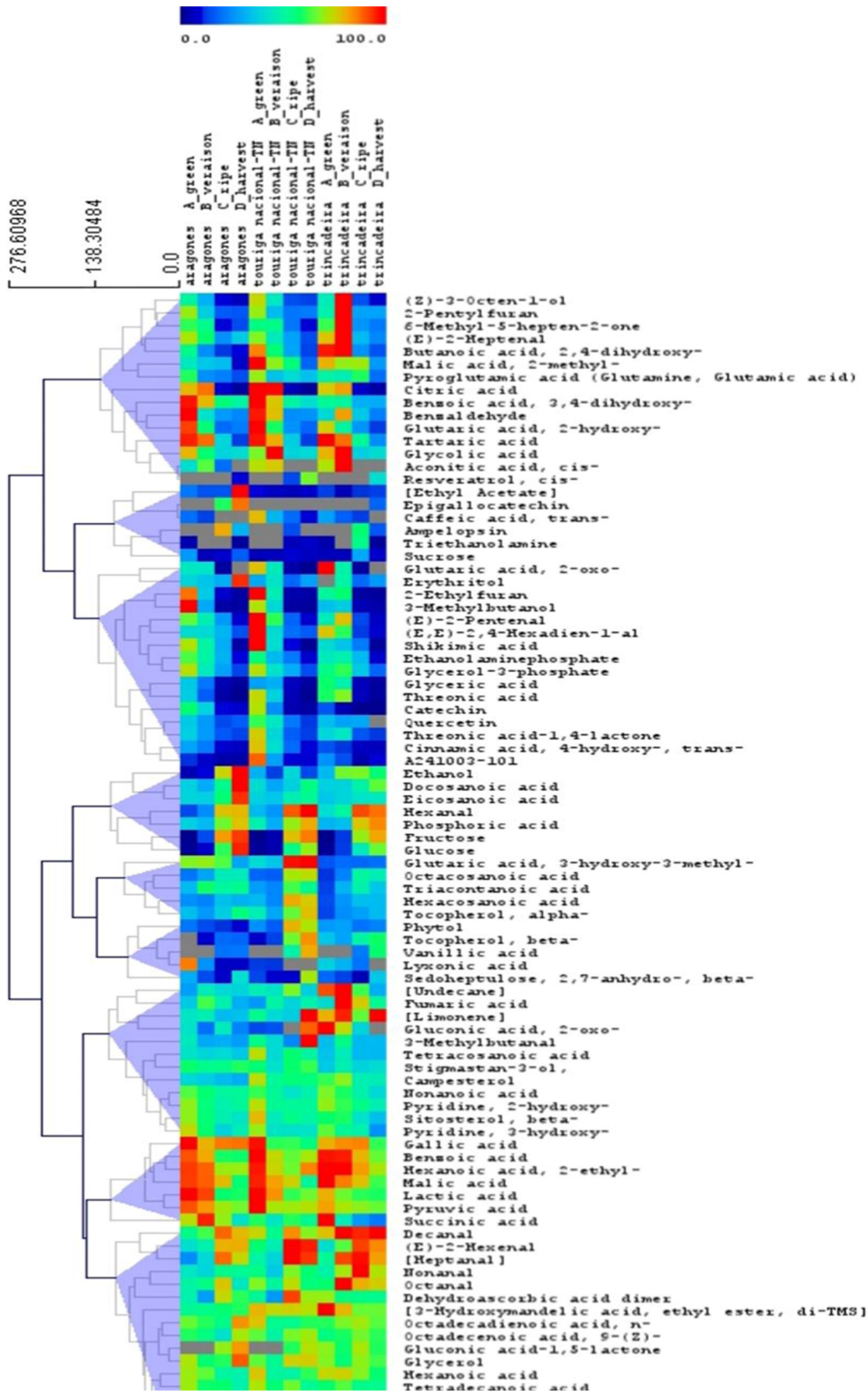


Figure 4. Heat map showing metabolite levels analyzed during berry ripening. Each square represents the average of the biological replicates.

doi:10.1371/journal.pone.0060422.g004

1282 and 954 probesets were down- and up- regulated, respectively (Table 2, File S3). The remaining 19 were either up- or down-regulated in the three varieties. The common set of modulated transcripts corresponds to 1915 unigenes.

Gene expression data of the three varieties were used for Multivariate Data Analysis using the Principal Component Analysis (PCA) (Fig. 5). A good discrimination was obtained regarding EL 35 and EL 36 stages for all the varieties through PC1 that accounts for 41,89% of the variance. On the other hand, PC2 that accounts for 26,27% of the variance enabled the discrimination of the varieties with Trincadeira clustering independently of the other varieties as obtained previously for metabolomics data.

Functional annotations could be assigned to the majority of probesets though 727 of the probesets had matches to genes with still unknown functions (Fig. 6). Eleven categories beside the genes with unknown function were differentially represented at significant levels during berry development in the common gene set. These were "primary metabolism", "secondary metabolism", "cellular metabolism", "development", "cellular process", "diverse functions", "regulation overview", "response to stimulus, stress", "signaling", "transport overview", and "xenoprotein, transposable element".

In order to validate microarray data and obtain further insights into expression of ten selected genes RT-qPCR analysis was performed (Fig. 7).

Analysis of gene expression and metabolite content during grape berry ripening

Carbohydrate metabolism. Berries start to accumulate after *véraison* the carbohydrates produced during photosynthesis and imported from the leaves.

Sucrose concentrations remained relatively constant with a slight increase towards harvest stage. This is in agreement with transcript abundance of a gene encoding an enzyme involved in sucrose biosynthesis that was higher at EL 36 when compared with EL35, namely sucrose phosphatase (VVTU21174_s_at, VIT_08s0032g00840) (Table 2).

A gene coding for a myb domain protein R1 transcription factor (VVTU2631_at, VIT_18s0001g09850) was up-regulated at EL 36 vs EL 35 in all varieties (File S3). This gene presents homology to one coding for a *Vitis vinifera* sucrose responsive element binding protein which represses sucrose transporters expression in grape berry [15]. This putative inhibition of sucrose transporters is in accordance with the fact that after *véraison* sucrose is no longer transported to the grape cells but instead hydrolyzed at the apoplast [16], which initiates a futile cycle of sucrose hydrolysis and resynthesis [17].

Furthermore, the transcript abundance of two vacuolar invertases, GIN1 and GIN2 (VVTU3710_at, VIT_02s0154g00090, VVTU13187_at, VIT_16s0022g00670), which catalyze the catabolism of sucrose to fructose and glucose, decreased during ripening (Table 2, File S3) as observed for Pinot Noir [7] and Syrah [18]. Proteomics data also showed decreased levels of these proteins in accordance with the relocation of sucrose hydrolysis from the vacuole to the apoplast after *véraison* [8].

As expected, at EL 35 an increase in fructose and glucose was already observed in all the varieties (File S2) confirming that the onset of *véraison* corresponds indeed to a stage of initiation of sugar accumulation. On the other hand, starch content has been shown

to decrease in Trincadeira berries at EL 35 and EL 36 [11]. However, genes putatively involved in synthesis of starch such as coding for Starch synthase 1, chloroplast precursor (VVTU3541_at, VIT_16s0098g01780) and starch synthase (VVTU13257_s_at, VIT_02s0025g02790) were up-regulated at EL 36 vs EL 35 in all varieties. On the other hand, a gene coding for an isoamylase-type starch-debranching enzyme 1 (VVTU13947_s_at, VIT_11s0078g00310) is down-regulated. This enzyme is assumed to play a role in biosynthesis of starch [19].

The control of activity of starch synthesis and starch degradation enzymes is complex in storage organs such as fruits. Different starch degradation pathways may be specific to early development and not active in late development [20].

We have observed a high up-regulation of a gene coding for galactinol synthase (VVTU3450_at, VIT_05s0020g00330) at EL 36 vs EL 35 (Table 2). The biosynthesis of raffinose and stachyose occurs via sequential transfers of galactosyl units to sucrose. The galactosyl donor is galactinol synthesized from UDP-galactose and myo-inositol, in a reaction catalyzed by galactinol synthase. The biosynthesis of raffinose and stachyose was reported during ripening of olive, also a non-climacteric fruit [21]. On the other hand, we observed up-regulation at EL 36 vs EL 35 of a gene coding for 1-phosphatidylinositol-4-phosphate 5-kinase (VVTU9324_at, VIT_18s0001g03290), an enzyme that participates in inositol phosphate metabolism and phosphatidylinositol signalling. It should be noted the considerable higher fold change displayed by the gene coding for galactinol synthase (VVTU3450_at, VIT_05s0020g00330) in Touriga Nacional (~105× comparing to 40.81× in Aragonês and 6.64× in Trincadeira). This may eventually imply a different composition in raffinose and stachyose for the three varieties. Raffinose is a minor carbohydrate in grape tissues but it has been reported that accumulation of raffinose in leaves of *Vitis vinifera* might be an early step of cold acclimation [22].

Interestingly, the sugar alcohol erythritol is more present in Aragonês cultivar at harvest stage, and may contribute to the final wine taste (File S2).

Plastid glycolysis seems to be inhibited at the onset and following *véraison* as we suggested previously [11]. On the other hand, cytoplasmic glycolysis seems to be activated. In fact, genes coding for pyruvate kinase, cytosolic isozyme (VVTU18887_s_at, VIT_08s0007g04170) are up-regulated at EL 36 vs EL 35 and a gene coding for a cytosolic fructose-1,6-bisphosphatase is down-regulated (VVTU12977_s_at, VIT_18s0072g00770). Although different berry tissues may have different trends of glycolysis [8], cellular compartmentation should be taken into account [11]. This subject deserves further confirmation as a marker of ripening. Nevertheless, the whole rate of glycolysis seems to decrease in ripe berries as suggested by the decrease in glyceric acid (File S2), a precursor of important biochemical intermediates in that process.

During ripening there is a major decrease in malate content as it was confirmed here by using GC-MS. The study of catabolism of this acid is very important for wine improvement due to its involvement in TCA cycle, gluconeogenesis, ethanol fermentation and for production of secondary metabolites (reviewed by [23]).

In the cytoplasm, malate can be produced from phosphoenolpyruvate produced in glycolysis through the activities of phosphoenolpyruvate carboxylase (PEPC) and malate dehydrogenase (MDH). One gene coding for a PEPC was down-regulated

Table 2. Selection of genes differentially expressed during ripening of the three grape varieties (considering a fold change ≥ 1.5 and FDR < 0.05 or fold change ≤ -1.5 and FDR < 0.05).

ProbeID	Trincadeira 2008	Touriga Nacional 2008	Aragonés 2008	Unique gene 12XID	Annotation
<i>CARBOHYDRATE, AMINO ACID AND LIPID METABOLISMS</i>					
WVTU12208_at	-3,56	-6,02	-3,1	VIT_01s0011g02740	Phosphoenolpyruvate carboxylase
WVTU12977_s_at	-2,59	-2,13	-2,26	VIT_18s0072g00770	fructose-1,6-bisphosphatase, cytosolic
WVTU13187_at	-22,87	-26,8	-33,59	VIT_16s0022g00670	vacuolar invertases, GIN2
WVTU13257_s_at	5,18	2,54	2,57	VIT_02s0025g02790	starch synthase
WVTU13533_s_at	1,85	1,55	1,56	VIT_16s0098g01200	6-phosphogluconolactonase
WVTU13825_at	-	2,05	2,26	VIT_02s0025g01410	Acyl-CoA synthetase long-chain member 2
WVTU1391_at	2,9	4,14	1,9	VIT_00s0391g00070	3-deoxy-D-arabino-heptulosonate 7-phosphate synthase
WVTU13947_s_at	-3,9	-2,6	-2,19	VIT_11s0078g00310	isoamylase-type starch-debranching enzyme 1
WVTU13950_s_at	-9,22	-20,03	-5,66	VIT_08s0007g07400	Glutamate dehydrogenase 1
WVTU15811_at	1,67	1,68	2,09	VIT_09s0002g00990	Triacylglycerol lipase
WVTU18887_s_at	1,74	1,83	1,54	VIT_08s0007g04170	pyruvate kinase, cytosolic isozyme
WVTU1903_at	-1,82	-1,89	-1,67	VIT_13s0019g05250	Malate dehydrogenase [NADP], chloroplast precursor (NADP-MDH)
WVTU21174_s_at	1,58	2,01	2,43	VIT_08s0032g00840	Sucrose-phosphatase
WVTU22296_s_at	-2,5	-2,34	-1,77	VIT_08s0040g03320	glutamate N-acetyltransferase
WVTU24552_at	-2,12	-3,73	-2,06	VIT_11s0016g00130	omega-6 fatty acid desaturase, chloroplast (FAD6) (FADC)
WVTU25722_at	2,84	2,15	2,45	VIT_18s0001g11910	1-acyl-sn-glycerol-3-phosphate acyltransferase 4
WVTU3450_at	6,64	104,86	40,81	VIT_05s0020g00330	galactinol synthase
WVTU3496_at	-2,49	-2,7	-3,21	VIT_01s0146g00070	11-beta-hydroxysteroid dehydrogenase
WVTU35040_s_at	-1,89	-2,21	-2,04	VIT_03s0038g00450	Squalene synthase
WVTU35129_s_at	10,64	11,55	10,6	VIT_18s0001g15460	stearyl acyl carrier protein desaturase
WVTU3541_at	2,45	2,62	2,18	VIT_16s0098g01780	soluble starch synthase 1, chloroplast precursor
WVTU35625_s_at	-2,5	-1,98	-2,01	VIT_19s0085g00880	succinate-semialdehyde dehydrogenase (SSADH1)
WVTU3709_at	3,04	1,79	3,29	VIT_09s0002g06970	Palmitoyl-monogalactosyldiacylglycerol delta-7 desaturase, chloroplast
WVTU3710_at	-3,03	-2,03	-5,65	VIT_02s0154g00090	vacuolar invertases, GIN1
WVTU37457_s_at	2,36	3,2	1,68	VIT_01s0127g00260	ATP-citrate synthase
WVTU3838_at	1,82	2,35	1,61	VIT_09s0018g01940	pyruvate dehydrogenase E1 component alpha subunit
WVTU40835_s_at	-	2,58	1,65	VIT_05s0020g03080	Acyl-CoA synthetase long-chain member 6
WVTU4095_at	-2,55	-4,9	-2,4	VIT_03s0088g01190	malate dehydrogenase, glyoxysomal precursor
WVTU4210_at	1,83	6,23	4,23	VIT_14s0068g01760	Alcohol dehydrogenase
WVTU5073_at	-2,14	-2,79	-3,29	VIT_08s0105g00430	omega-3 fatty acid desaturase, chloroplast precursor
WVTU5906_at	1,62	3,65	3,15	VIT_07s0031g02840	Diacylglycerol kinase 2
WVTU6948_at	1,53	6,69	3,19	VIT_04s0008g06570	chorismate mutase, cytosolic (CM2)
WVTU8069_at	-2,01	-2,32	-2,18	VIT_08s0007g05710	L-Galactono-1,4-lactone dehydrogenase
WVTU8356_at	5,11	10,04	4,14	VIT_07s0005g01240	triacylglycerol lipase
WVTU9324_at	1,52	1,52	2,35	VIT_18s0001g03290	1-phosphatidylinositol-4-phosphate 5-kinase
WVTU9635_s_at	-3,06	-4	-2,9	VIT_03s0038g02510	glyoxylate reductase
WVTU9987_s_at	-3,41	-2,23	-2,84	VIT_05s0020g04510	GDP-mannose 3,5-epimerase 1
<i>FLAVONOID AND STILBENE METABOLISMS AND AROMA DEVELOPMENT</i>					
WVTU11834_at	2,72	3,83	3,03	VIT_09s0002g06420	Lactoylglutathione lyase
WVTU11927_at	2,7	10,66	2,9	VIT_05s0062g00980	aldo/keto reductase AKR
WVTU12032_s_at	6,62	7,34	2,89	VIT_06s0004g08150	trans-cinnamate 4-monooxygenase
WVTU13018_s_at	-	-	1,57	VIT_15s0046g02300	Beta-cyanoalanine synthase

Table 2. Cont.

ProbeID	Trincadeira 2008	Touriga Nacional 2008	Aragonès 2008	Unique gene 12XID	Annotation
WVTU13618_x_at	-2,1	-3,21	-2,03	VIT_16s0050g01580	UDP-glucose: anthocyanidin 5,3-O-glucosyltransferase
WVTU13738_at	-5,78	-6,69	-6,79	VIT_16s0050g01090	Beta-carotene hydroxylase
WVTU13791_at	-	2,57	-	VIT_02s0025g00240	Beta-carotene hydroxylase
WVTU13955_at	1,69	2,64	-	VIT_14s0128g00780	lipoxygenase
WVTU14620_at	1,79	6,38	3,66	VIT_18s0041g00740	UDP-glucose: anthocyanidin 5,3-O-glucosyltransferase
WVTU14878_s_at	-	3,53	-	VIT_04s0023g02200	S-adenosyl-L-methionine:salicylic acid carboxyl methyltransferase
WVTU15353_at	4,04	12,57	2,7	VIT_11s0065g00350	trans-cinnamate 4-monooxygenase
WVTU15628_s_at	6,01	29,77	4,29	VIT_16s0100g00950	Stilbene synthase 3
WVTU16103_at	1,54	3,68	2,03	VIT_18s0001g03470	Flavonol synthase
WVTU16622_at	258,59	46,4	16,14	VIT_00s0225g00230	alliin lyase precursor
WVTU17111_s_at	-1,63	-1,97	-1,71	VIT_03s0180g00200	Limonoid UDP-glucosyltransferase
WVTU17555_s_at	-4,68	-	-	VIT_10s0003g03750	9-cis-epoxycarotenoid dioxygenase 2
WVTU21329_at	9,32	3,43	1,99	VIT_16s0039g00880	CYP89H3
WVTU21725_at	-	3,24	2,79	VIT_15s0046g03600	(+)-neomenthol dehydrogenase
WVTU2626_at	-	2,57	-	VIT_17s0000g05580	isopiperitenol dehydrogenase
WVTU34553_s_at	6,36	33,68	4,42	VIT_16s0100g01030	stilbene synthase [<i>Vitis quinquangularis</i>]
WVTU34913_at	3,25	8,38	1,81	VIT_16s0100g00810	stilbene synthase [<i>Vitis vinifera</i>]
WVTU3533_s_at	11,83	5,84	2,04	VIT_05s0077g01300	Aldo-keto reductase
WVTU35884_at	2,73	-	-	VIT_06s0009g03010	flavonoid 3',5'-hydroxylase [<i>Vitis vinifera</i>]
WVTU36515_at	-4,79	-	-2,73	VIT_00s0271g00030	myrcene synthase
WVTU36927_x_at	-14,1	-3,01	-4,28	VIT_12s0059g01790	Caffeic acid O-methyltransferase
WVTU37595_s_at	-	-	-1,82	VIT_12s0059g01060	hydroperoxide lyase (HPL1)
WVTU39097_at	-2,47	-3,28	-3,79	VIT_04s0079g00680	phytoene synthase, chloroplast precursor
WVTU4228_at	-	1,7	-	VIT_14s0030g01740	Zeta-carotene desaturase ZDS1
WVTU4697_at	-6,77	-10,64	-9,48	VIT_08s0007g01040	aldo-keto reductase
WVTU5363_at	8,86	7,98	6,35	VIT_09s0018g01490	Anthraniloyl-CoA: methanol anthraniloyl transferase
WVTU5372_s_at	-3,83	-2,78	-2,53	VIT_04s0023g02280	S-adenosyl-L-methionine:salicylic acid carboxyl methyltransferase
WVTU6355_at	-3,24	-4,38	-3,08	VIT_07s0031g00620	zeaxanthin epoxidase (ZEP) (ABA1)
WVTU7133_s_at	-5,94	-9,97	-4,21	VIT_15s0046g03570	(+)-neomenthol dehydrogenase
WVTU8254_at	-	2,79	-	VIT_02s0087g00930	9-cis-epoxycarotenoid dioxygenase
WVTU8882_at	7,64	-	7,85	VIT_01s0011g05920	S-adenosyl-L-methionine:salicylic acid carboxyl methyltransferase
WVTU9837_s_at	-2,05	-2,04	-2,4	VIT_04s0008g03560	lactoylglutathione lyase
WVTU9888_at	-2,28	-3,28	-2,1	VIT_05s0049g01130	aldo/keto reductase

doi:10.1371/journal.pone.0060422.t002

(VVTU12208_at, VIT_01s0011g02740) at EL 36 vs EL 35 together with two genes coding for malate dehydrogenase (VVTU1903_at, VIT_13s0019g05250, VVTU4095_at, VIT_03s0088g01190) in agreement with a decrease in malate. Two of these genes (VVTU12208_at, VIT_01s0011g02740, VVTU4095_at, VIT_03s0088g01190) were more down-regulated in Touriga Nacional (Table 2) which may be related to an enhanced decrease in malic acid content of this variety at EL 38 (Fig. 2).

It is not surprising that a gene coding for a TONOPLAST DICARBOXYLATE TRANSPORTER with homology to a

sodium-dicarboxylate cotransporter (VVTU17663_s_at, VIT_00s2188g00010), which is putatively involved in the transport of malate in the vacuole, was down-regulated at EL 36 vs EL 35 (File S3).

Organic acids such as malic and tartaric acids are well known for their contribution to wine taste. At *véraison* large amounts of malate released from the vacuole may be directly transported to the mitochondria and fed into an increased TCA cycle flux.

The mitochondrial pyruvate dehydrogenase complex provides acetyl-CoA for the TCA cycle and NADH for oxidative phosphorylation. The alpha (VVTU3838_at,

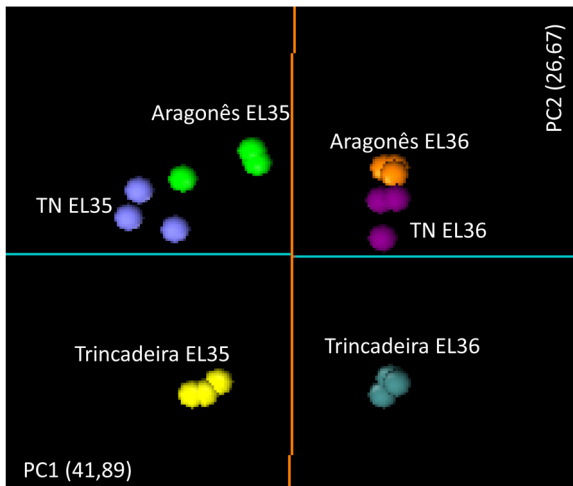


Figure 5. PCA plot showing transcriptional discrimination of developmental stages and cultivars. The first (PC1) and the second (PC2) principal components are represented. doi:10.1371/journal.pone.0060422.g005

VIT_09s0018g01940) subunit of the pyruvate dehydrogenase complex was induced after *véraison*, though this enzyme is known to be highly regulated post-translationally.

We observed an increase in the expression of a gene coding for ATP-citrate synthase (VVTU37457_s_at, VIT_01s0127g00260) at EL 36 vs EL 35 in all varieties though the highest level of expression was observed in Touriga Nacional. At EL 32 and EL35 this variety tends to present more citric acid than Aragonês and Trincadeira. Aragonês showed elevated concentration of succinate whereas Trincadeira of fumarate (File S2).

While malic and tartaric acids showed the highest content in green berries in all varieties, citrate, succinate and fumarate showed the highest content in different developmental stages (green or *véraison*) depending on the variety. During ripening a transcript encoding a Succinic semialdehyde dehydrogenase (SSADH1; VVTU35625_s_at, VIT_19s0085g00880) putatively involved in succinate synthesis is down-regulated in all varieties as obtained by both microarray and RT qPCR analysis (Fig. 6). It was also noticed that several genes coding for enzymes of the TCA cycle such as aconitate hydratase and malate dehydrogenase showed different expression among the three varieties, being some genes up or down-regulated in one variety but not in other (File S3).

The increase in the rate of glycolysis due to an excess of sugars leads to an increase in pyruvate that may trigger aerobic fermentative metabolism [24].

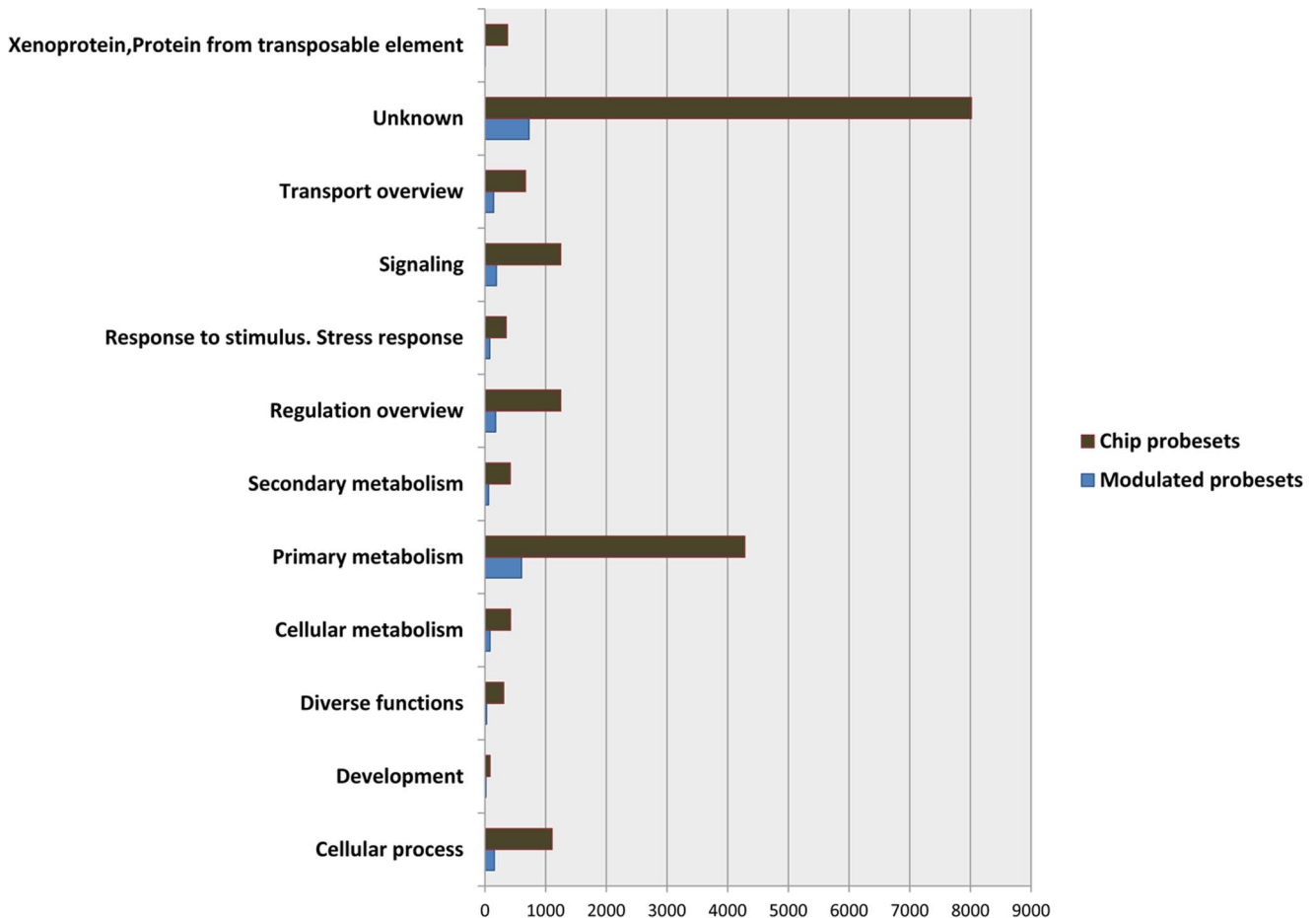


Figure 6. Functional categories distribution in the common gene set of the 2255 modulated probesets and in the entire GrapeGen Chip®. doi:10.1371/journal.pone.0060422.g006

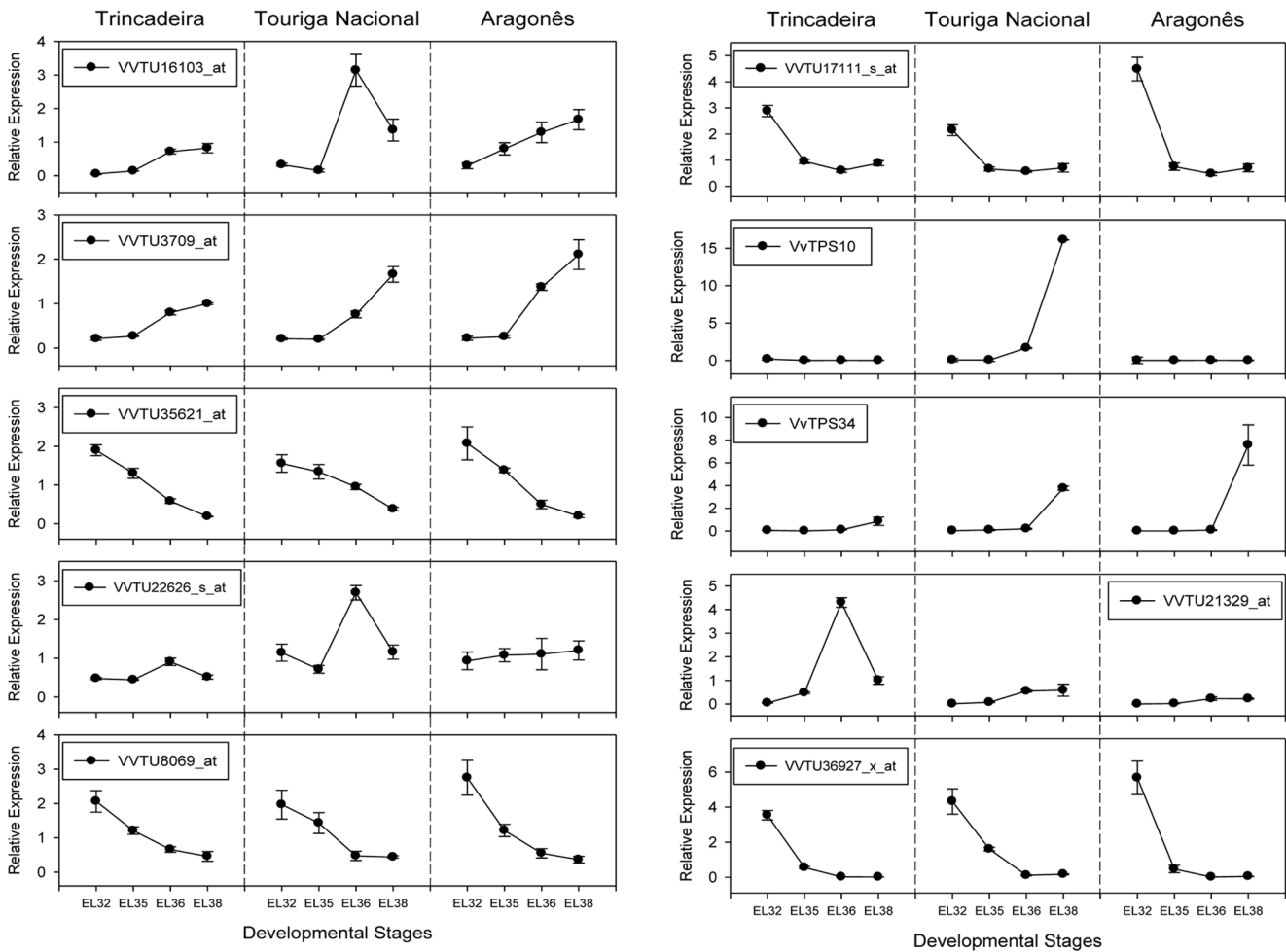


Figure 7. Real time qPCR validation of the expression profiles of ten genes in the three varieties under analysis. Data are reported as means \pm SE of three technical and two-three biological replicates. Transcript levels were calculated using the standard curve method and normalized against grapevine actin gene (VVTU17999_s_at) used as reference control. Flavonol synthase (VVTU16103_at); Palmitoyl-monogalactosyldiacylglycerol delta-7 desaturase, chloroplast (VVTU3709_at); Succinate semialdehyde dehydrogenase (VVTU35625_s_at); Tocopherol cyclase (VVTU22626_s_at); L-Galactono-1,4-lactone dehydrogenase (VVTU8069_at); Limonoid UPD-glycosyltransferase (VVTU17111_s_at); Terpene synthase (VvTPS10); Terpene synthase (VvTPS34); Cytochrome 450 monooxygenase CYP89H3 (VVTU21329_at) and Caffeic acid O-methyltransferase (VVTU36927_x_at). doi:10.1371/journal.pone.0060422.g007

In fact, the production of ethanol by pyruvate decarboxylase and alcohol dehydrogenase may occur in ripening fruit [23]. Here it was observed an increase in ethanol during ripening in all varieties though pyruvate levels showed no significant change. It was observed up-regulation at EL 36 vs EL 35 of genes coding for alcohol dehydrogenase and aldehyde dehydrogenase [7] which may be indicative of a shift to an aerobic fermentative metabolism during ripening [25].

We observed that a gene coding for an Alcohol dehydrogenase (VVTU4210_at, VIT_14s0068g01760) was up-regulated at EL 36 vs EL 35. This data may indicate that aerobic fermentation is occurring during ripening of all varieties. Other genes coding for alcohol dehydrogenases were up- or down-regulated in only one or two varieties (File S3). Interestingly, acetic acid, a product of ethanol metabolism which is known for giving a sour, pungent fatty and sweaty aroma to wines was previously detected in higher amounts at harvest stage (EL 38) in Trincadeira comparing to the other varieties Aragonês and Touriga Nacional [13].

There is a general tendency for an increase in dehydroascorbic acid dimer (an oxidized form of ascorbic acid) at EL 36 and EL 38. This is not surprising since ripening is characterized by increased

oxidative stress [7,11]. Moreover, ascorbic acid present in abundant amounts in fruits undergoes rapid oxidation to dehydroascorbic acid [26] yielding reduced glutathione. Previously, the content in glutathione was shown to increase during grape ripening with 90% being reduced [27] in agreement with these results. Moreover, ascorbate was shown to decrease during ripening [11] together as indicated here with genes coding for GDP-mannose 3,5-epimerase 1 (VVTU9987_s_at, VIT_05s0020g04510), VTC2 (VITAMIN C DEFECTIVE), L-Galactono-1,4-lactone dehydrogenase (VVTU8069_at, VIT_08s0007g05710), enzymes putatively involved in ascorbate biosynthesis. At the same time there is a decrease in threonic acid (File S2) which is a polyhydroxy acid derived from L-ascorbic acid [28].

The pentose phosphate pathway is a process that generates NADPH and pentoses used in reductive biosynthesis reactions within cells (e.g. fatty acid synthesis). An increase in expression of a gene coding for 6-phosphogluconolactonase (VVTU13533_s_at, VIT_16s0098g01200) at EL 36 vs EL 35 in all varieties from the pentose phosphate pathway may be related to increase in fatty acids content as it will be discussed in paragraph on lipid

metabolism. Interestingly, there is a big increase in β -sedoheptulose at EL 38 in agreement with major fatty acid accumulation.

In conclusion, the analysis of expression of genes involved in carbohydrate metabolism and contents in metabolites in all varieties indicates that *véraison* is a stage of active carbohydrate metabolism and transport. Ripening is characterized by a complex mechanism of starch breakdown with little sucrose accumulation but major accumulation of fructose and glucose. Raffinose and stachyose may play an important role in ripening of grapes. On the other hand, the pentose phosphate pathway seems to be involved in grape ripening together with aerobic fermentative metabolism. The TCA cycle may operate differently among the varieties since they were accumulating different contents in organic acids in particular in pre-*véraison* and *véraison* stages.

Lipid metabolism. The glyoxalate cycle plays a role in metabolism of fatty acids during seed germination; but was relevant to our analyses even though seeds have been removed from our samples. At EL 36 vs EL 35 there is down-regulation of a gene coding for glyoxalate reductase (VVTU9635_s_at, VIT_03s0038g02510) in all varieties in agreement with a decrease in glycolic acid (Tables 1, 2). The net result of the glyoxalate cycle is the production of glucose from fatty acids. However, fatty acid oxidation does not seem to be favored during ripening in pulp and skin but instead fatty acid biosynthesis appeared to be enhanced. Indeed, we have observed at EL 36 and EL 38 an increase in content in several saturated fatty acids (Table 1, File S2) as previously reported for another *Vitis vinifera* variety [29]. Moreover, genes coding for key enzymes of glyoxalate cycle such as malate synthase and isocitrate lyase were down-regulated though not in all varieties (File S3).

It was observed up-regulation at EL 36 vs EL 35 of two genes coding for Acyl-CoA synthetase long-chain member 2 and 6 (VVTU13825_at, VIT_02s0025g01410, VVTU40835_s_at, VIT_05s0020g03080) in Touriga Nacional and Aragonês. The skin of berries from these varieties is thicker than from Trincadeira (Agudelo-Romero et al., unpublished). Fatty acids can be found in cells in activated form performed by enzymes acyl-CoA synthetases. The resultant acyl-CoAs are used in the biosynthesis of many cellular products such as wax and cutin which are components of berry skins. After *véraison* grape berries continue to enlarge due to cell expansion driven by the increase of sugar content in the cell vacuole and a continuous flow of water; therefore a thick cuticle is necessary to avoid evapotranspiration.

The surface wax of the grape berry is chemically a mixture of long-chain alcohols, esters of such alcohols and fatty acids, free fatty acids, long-chain aldehydes, and hydrocarbons [30]. The GC-MS platform enabled the identification of several saturated fatty acids which in general increase at EL 36 and/or EL 38, namely octacosanoic, hexacosanoic and triacontanoic acids (Table 1, File S2). This increase was much more noticed in Touriga Nacional berries whereas docosanoic and eicosanoic acids showed increased levels at EL 38 in Aragonês cultivar. This increase is not surprising since saturated long-chain fatty acids are major constituents of grape waxes that accumulate in ripe berries. The hexacosanoic acid or cerotic acid is a component of carnauba wax, an extremely good wax presenting several commercial applications. It is interesting to note that this fatty acid increased significantly in Touriga Nacional samples (File S2). The composition of their skin e.g wax density may influence the resistance of this variety to fungal attack [31] comparing to other varieties such as Trincadeira.

Lipid components in fruits though occurring in low amounts are important due to their nutritional value and due to their contribution to aroma and flavor. Fatty acids as n-hexadecanoic

acid and 9,12-(Z, Z)-octadecadienoic acid (linoleic acid) have an important influence on the flavour of strawberry fruit [32].

A gene coding for a chloroplastidial omega 6-fatty acid desaturase (VVTU24552_at, VIT_11s0016g00130) was down-regulated at EL 36 vs EL 35 in all the varieties. This enzyme also known as FAD6 is the primary route of polyunsaturated fatty acids production in plants and converts oleic acid (18:1, a monounsaturated fatty acid) to linoleic acid [33] which provides a potential herbaceous aroma in ripe grapes [29]. In fact, we did not detect a significant decrease in linoleic acid. Also a gene coding for a chloroplastidial omega-3 fatty acid desaturase (VVTU5073_at, VIT_08s0105g00430) putatively involved in α -linolenic acid biosynthesis is down-regulated at EL 36 vs EL 35 in all varieties.

A gene coding for a stearyl acyl carrier protein desaturase was up-regulated at EL 36 vs EL 35 in all varieties (VVTU35129_s_at, VIT_18s0001g15460). Stearoyl ACP-desaturase, commonly known as fatty acid biosynthesis 2 (FAB2), is a key enzyme that catalyzes the conversion of stearic (18:0) into oleic acid (18:1) [34]. Nevertheless we did not observe a significant decrease in stearic acid also known as octadecanoic acid. Other fatty acids such as octadecenoic and hexadecanoic also showed no significant differences throughout ripening (File S2). However, in 'Pedro Ximnez' *Vitis vinifera* grapes hexadecanoic acid (palmitic acid) increased during ripening [29] highlighting metabolic specificities among varieties.

Regarding steroid biosynthesis we have observed down-regulation of genes coding for squalene synthase (VVTU35040_s_at, VIT_03s0038g00450), and 11- β -hydroxysteroid dehydrogenase (VVTU3496_at, VIT_01s0146g00070) suggesting decreased steroid synthesis at EL 36. In fact, a transcript encoding 11- β -hydroxysteroid dehydrogenase has been recently considered a biomarker of pre-*véraison* and *véraison* stages [9]. Campesterol decreased during ripening in all the varieties while stigmastan-3-ol showed no significant variation in content.

In tomato, among all sterol lipids, the ratio of stigmasterol to β -sitosterol the two major sterols in tomato, increased 2.3-fold during ripening [35]. It has been reported an increase in the total sterol content of pericarp tissue during ripening of tomato fruit from mature green to red ripe stages [36]. In berries of *Vitis vinifera* at least for the sterols evaluated this does not seem to be the case. In addition, a gene involved in brassinosteroids biosynthesis from campesterol and coding for a steroid 5 alpha reductase DET2 (VVTU6606_at, VIT_08s0007g01760) was down-regulated at EL 36 vs EL 35 in all the varieties (File S3). This class of hormones plays an important role in the onset of grape ripening [37].

We observed an increase in α -tocopherol and β -tocopherol in all varieties during ripening but in particular in Touriga Nacional. The increase in tocopherol has been reported also for tomato and recently shown to be regulated by *APETALA2a* (*AP2a*) transcription factor [38]. It is interesting to note that a gene coding for *AP2a* (VVTU2494_at, VIT_07s0031g00220) was up-regulated at EL 36 vs EL 35 in all the varieties (File S3). It remains to be established whether this transcription factor is a major regulator of grape ripening as occurs in tomato [38].

The increase was mostly noticed for α -tocopherol which presents the highest anti-oxidant activity. Previously, we reported an increase in glutathione during ripening of Trincadeira grapes and suggested to be related to increased oxidative stress at the onset of ripening and during ripening as suggested by [7]. Interestingly, we observed up-regulation in Touriga Nacional and Trincadeira at EL 36 vs EL 35 of a gene coding for tocopherol cyclase (VVTU22626_s_at, VIT_04s0008g03600, File S3) which catalyzes the penultimate step of tocopherol synthesis. The

precursor of tocopherol, phytol also increases at EL 36 and EL 38 in Touriga Nacional berries.

Derivatives of fatty acids may be structural components of cell membranes, and/or used in triacylglycerol production [39]. Two genes coding for triacylglycerol lipases (VVTU15811_at, VIT_09s0002g00990, VVTU8356_at, VIT_07s0005g01240) were up-regulated at EL 36 vs EL 35, and may be involved in the release of fatty acids. The resultant product of glycerol-3-phosphate which decreases during ripening (File S2) may be metabolized for synthesis of esters of fatty acids for surface waxes [40,41]. It was noticed an up-regulation of a gene coding for chloroplastidial palmitoyl-monogalactosyldiacylglycerol delta-7 desaturase in all the varieties up to EL 38 as revealed by RT qPCR data (VVTU3709_at, VIT_09s0002g06970, Fig. 7) putatively involved in unsaturated fatty acid biosynthesis for that purpose. Interestingly, glycerol which is also important for wines taste presented the highest concentration at EL 38 in Aragonês (File S2).

On the other hand, it was noticed the up-regulation of a gene coding for a diacylglycerol kinase 2 (VVTU5906_at, VIT_07s0031g02840) which functions in the recycling of diacylglycerol, yielding phosphatidic acid, a compound that has emerged as an important lipid second messenger in plants, being involved in a wide range of biotic (e.g. pathogens) and abiotic (e.g. osmotic, temperature) stress responses [42]. These stresses are known to increase during grape ripening [11].

It was observed the up-regulation at EL 36 vs EL 35 in all varieties of a gene coding for a 1-acyl-sn-glycerol-3-phosphate acyltransferase (VVTU25722_at, VIT_18s0001g11910) which intervenes in the phospholipid biosynthetic process. This suggests that this class of lipids may increase during ripening as it occurs with *Capsicum annuum*, another non-climacteric fruit [43]. Indeed, the most abundant fraction of grape lipids has been reported to be the phospholipids [44].

The metabolism of lipids is very active during grape ripening due to the breakdown of plastid thylakoids, and differentiation of chloroplasts into non-photosynthetic chromoplasts. In these plastids fatty acid biosynthesis is enhanced for wax biosynthesis, as well as for aroma production which is due also to a specific fatty acid and correspondent esters combination. Steroid composition also varies among varieties but tends to decrease during ripening. On the contrary, tocopherol increases probably to cope with increased stress occurring during grape ripening.

Amino acid metabolism. Homoserine and pyroglutamic acid which when monitored by the chosen GC-MS profiling approach also includes glutamine and glutamic acid were the amino acids identified (Table 1). In this context, the use of an NMR-based platform enabled the quantification of many amino acids, namely arginine, valine and threonine [13]. This highlights the fact that both platforms used in metabolomics studies are complementary. Glutamate was shown previously to decrease at EL 38 in all varieties [13] as it happens here with pyroglutamic acid.

It is interesting to note that genes related to glutamate metabolism were down-regulated at EL 36 vs EL 35 in all the varieties and may eventually be considered as negative markers of ripening such as glutamate N-acetyltransferase (VVTU22296_s_at, VIT_08s0040g03320) and glutamate dehydrogenase 1 (VVTU13950_s_at, VIT_08s0007g07400).

L-Homoserine is a precursor of methionine biosynthesis. Interestingly, it has been shown that homoserine accumulation in the chloroplast triggers a novel form of downy mildew resistance that is independent of known defense signaling pathways [45]. Though the levels of this amino acid have remained the same

throughout ripening in all varieties we have detected increased methionine levels towards harvest especially in Trincadeira [13].

S-adenosyl-L-methionine is a precursor of both ethylene and polyamine biosynthesis. Recently, we showed that during ripening there is an increase in polyamine catabolism in the three varieties [46].

Regarding the synthesis of aromatic amino acids such as phenylalanine which is a precursor of the phenolic compounds that accumulate during ripening, it was observed the up-regulation at EL 36 vs EL 35 of genes coding for a 3-deoxy-D-arabino-heptulosonate 7-phosphate synthase (VVTU1391_at, VIT_00s0391g00070) and a cytosolic chorismate mutase (VVTU6948_at, VIT_04s0008g06570) putatively involved in shikimate metabolism and phenylalanine biosynthesis. Therefore, it is not surprising that shikimate content is decreased in berries at ripe and harvest stages (File S2) though it was substantially higher at EL 32 and EL 35 in Aragonês and Touriga Nacional cultivars than in Trincadeira. Those varieties are known to accumulate more phenolic compounds [13]. Also different genes coding for phenylalanine ammonia lyase were up-regulated at EL 36 vs EL 35 though not in all varieties (File S3).

From the above it can be suggested that the metabolisms of glutamate, methionine and phenylalanine play a major role in grape ripening.

Flavonoid and stilbene metabolism. Genes coding for enzymes acting on flavonols, stilbenes, and anthocyanins synthesis were noticed to be induced during grape ripening [7,11]. Our results confirm these for all the varieties and establish these genes as candidate markers of grape ripening. In addition, many genes coding for transcription factors of the MYB family were up-regulated at EL 36 vs EL 35 in all the varieties and may be involved in the regulation of the flavonoid pathway as other previously characterized MYB transcription factors [12]. These are the case of genes coding for myb domains proteins 73, 14, R1 and 94 (File S3).

A gene coding for a flavonol synthase (VVTU16103_at, VIT_18s0001g03470) was up-regulated at EL36 vs EL 35. This enzyme is responsible for the conversion of dihydroflavonols to flavonols which are important co-pigments that stabilize anthocyanins in wine. In the skin of Shiraz berries, *VvFLS1* expression is highest between flowering and fruit set, then declines to *veraison*, and increases again during ripening coincident with accumulation of flavonols per berry [47]. The same seems to be the case of this gene coding for flavonol synthase at least in Touriga Nacional (Fig. 7).

However, in this work it was detected a decrease in quercetin following EL 32 in all varieties including Touriga Nacional (Fig. 8) in agreement with a previous identified decrease in quercetin glycoside using NMR [13]. Ampelopsin or dihydromyricetin is a flavanone presenting anti-cancer properties and derives from the flavonol myricetin [48]. Interestingly, it was detected at higher concentrations in ripe berries (EL 36) (Fig. 8) and mainly in Aragonês. This fact highlights the use of GC-MS as a platform to investigate the medicinal potential of samples.

A reduction in tannin concentration from pre-*veraison* to harvest has been well documented [49]. The tannin catechin decreases during ripening in all varieties as shown in Fig. 8 for Touriga Nacional. However, it should be noted that Trincadeira presents much lower levels of catechin at EL 32 and EL 35 than the other varieties. Interestingly, epigallocatechin was higher in Aragonês at harvest stage and may contribute to higher astringency of the wine. This compounds is a precursor of epigallocatechin-3-gallate which is known for the anti-oxidant properties [50]. The observed

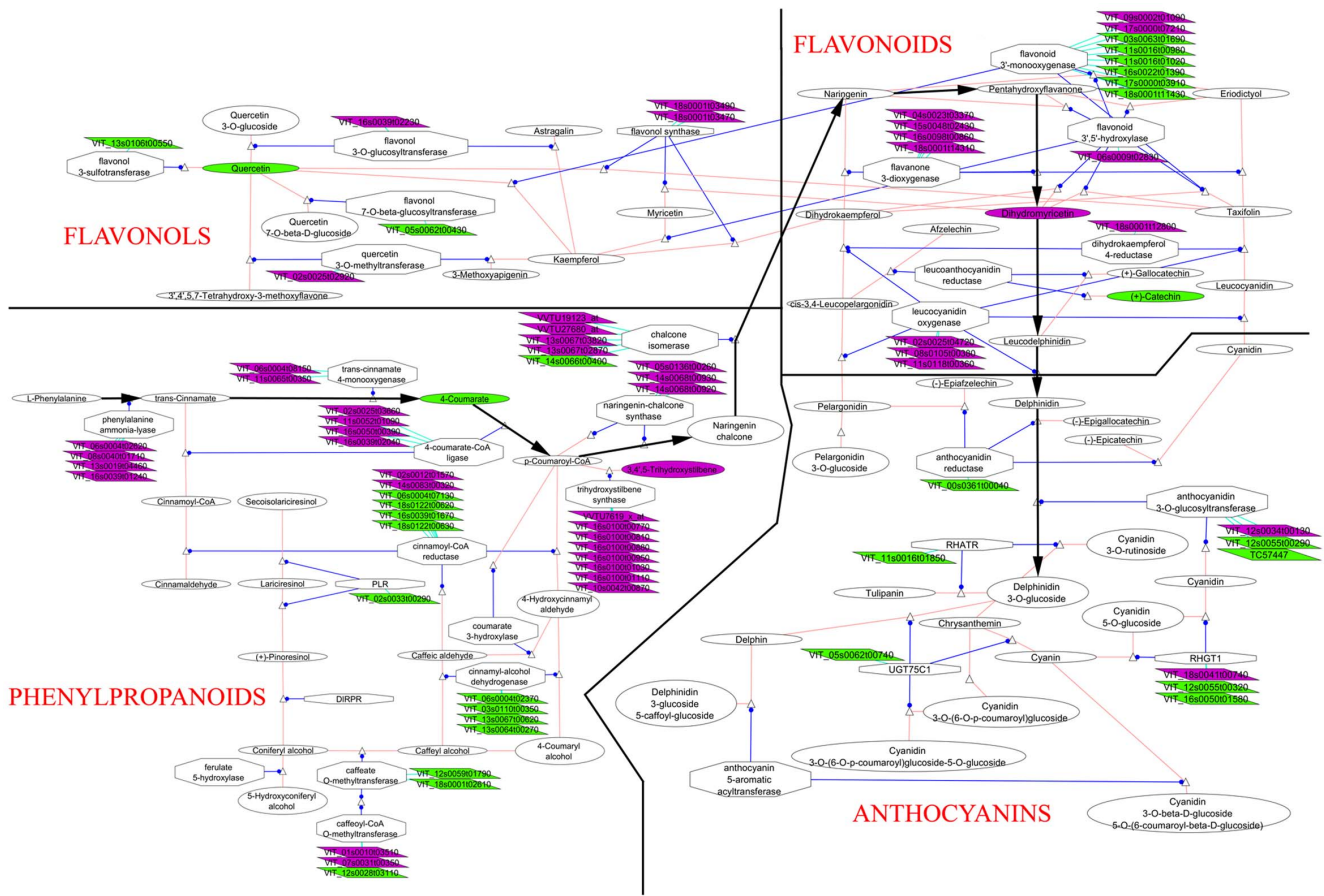


Figure 8. Phenylpropanoids-related transcripts and metabolites showing significant differences between véraison and ripening (EL 36 vs EL 35) in Touriga Nacional cultivar; pathways are represented in VitisNet networks [81] with the Cytoscape software. Parallelograms represent non-redundant transcripts differentially expressed. Ovals and hexagons represent metabolites and enzymes, respectively. Pink lines show metabolic reactions and blue lines catalytic reactions; bold arrows highlight the reactions starting from phenylalanine leading to anthocyanidin biosynthesis. Green represents transcripts down-regulated or decrease in metabolites values, whereas purple represents transcripts up-regulated or increase in metabolites values. doi:10.1371/journal.pone.0060422.g008

decrease in gallic acid during ripening is expected since this compound makes part of tannins such as epigallocatechin.

It is clear the overall flavonoid profile of grapes changes significantly over time [51] and includes a significant reduction in catechin and gallic acid.

One gene coding for an UDP-glucose: anthocyanidin 5,3-O-glucosyltransferase (VVTU14620_at, VIT_18s0041g00740) was up-regulated at EL36 vs EL 35. Another gene coding for this enzyme was down-regulated (VVTU13618_x_at, VIT_16s0050g01580) at EL 36 when compared to EL 35 but was up-regulated at EL 35 when compared to EL 32 at least for Trincadeira cultivar [11]. This suggests that the pattern of anthocyanins may change during berry ripening as recently observed for Corvina berries [51].

These authors showed a rapid accumulation of nonacylated anthocyanins and flavones during véraison, concomitant with a sharp decline in the levels of aromatic organic acids and procyanidins. This could be due to the use of the organic acid pool to provide precursors for the synthesis of other molecules. For example, both coumaric acid and caffeic acid could in principle be used (as coumaroyl-CoA and caffeoyl-CoA, respectively) as substrates for the production of chalcones by chalcone synthase. The resulting chalcones could then be used for the synthesis of

flavones and anthocyanins [51]. Interestingly, we have detected a decrease in caffeic acid in ripe berries of all the varieties being no longer detected at harvest stage. Touriga Nacional was the variety accumulating more caffeic acid at EL 32 and shown to present more anthocyanins at EL 36 and EL 38 (Fig. 1). The same holds true for trans- 4-hydroxycinnamic acid or *p*-coumaric acid (Fig. 8), which is a precursor of flavonoids, stilbenes and coumarins [52]. Two genes coding for trans-cinnamate 4-monoxygenase (VVTU15353_at, VIT_11s0065g00350, VVTU12032_s_at, VIT_06s0004g08150) were more expressed at EL 36 vs EL 35 in Touriga Nacional (Fig. 8). Previously, and through an NMR platform it was established that the green and véraison stages (EL 32, EL 35) of Touriga Nacional presented more hydroxycinnamic acid derivatives such as caftaric acid than Aragonés and Trincadeira [13] and that was recently related to increased antitumoral properties of that cultivar [53].

One gene coding for flavonoid 3,5 -hydroxylase (VVTU35884_at, VIT_06s0009g03010) was up-regulated at EL 36 vs EL 35 but only in Trincadeira (Table 2, File S3). This enzyme catalyzes the hydroxylation of the B-ring of flavonoids and can act on flavonols, anthocyanins, and proanthocyanidins. Bogs and co-workers [54] showed that in berry skin, expression of these genes was low at the onset of ripening but increased after véraison

concomitant with the accumulation of 3'- and 3',5'-hydroxylated anthocyanins. The hydroxylation pattern of the B-ring is an important determinant of flavonoids coloration, stability, and antioxidant capacity [55].

Regarding stilbenes, their accumulation during ripening of grape berries is well known [2]. It is interesting to note, however, that resveratrol or *trans*-3, 4',5,-trihydroxystilbene is present at higher concentrations in Touriga Nacional berries at ripe (Fig. 8) and harvest stages in agreement with a higher fold change detected at EL 36 vs EL 35 in this variety for several genes coding for stilbenes synthases (VVTU34913_at, VIT_16s0100g00810, VVTU15628_s_at, VIT_16s0100g00950, VVTU34553_s_at, VIT_16s0100g01030).

Phenylpropanoid metabolism plays a major role in grape ripening changing the content in hydroxycinnamic acid derivatives, flavonols, tannins, anthocyanins, and stilbenes from green to harvest stage of grapes and presenting cultivar specific variation with a tendency of Touriga Nacional to present more phenolics.

Aroma development

Monoterpenes, C₁₃-norisoprenoids, and some benzenoid compounds are the most important grape aroma substances present in the pulp and skin of berries in both free and glycoside forms. Their specific profiles depend mainly on the variety though environmental cues may have impact (Flamini and Traldi, 2010).

The largest class of plant volatiles is derived from isoprenoid pathways [56]. The mevalonate pathway is a source of isoprene units for the biosynthesis of cytokinins and brassinosteroids. In plants, both the cytosolic mevalonate and the plastidic methylerythritol phosphate pathways generate the five-carbon compound isopentenyl pyrophosphate and its isomer dimethylallyl pyrophosphate. These two precursors give rise to volatile and non-volatile terpenoid compounds such as monoterpenes (C₁₀), sesquiterpenes (C₁₅) diterpenes (C₂₀), triterpenes (C₃₀), carotenoids, sterols and phytols. In this respect, it should be noted that Touriga Nacional presented a higher quantity of phytol at EL 36 and EL 38 than Aragonês and Trincadeira.

Variety, *terroir*, sunlight exposure, soil water retention capacity as well as ripening stage affect carotenoid concentration in the grapes which is known to decrease following *véraison* [57]. So it is not surprising that genes coding for a chloroplast precursor of phytoene synthase (VVTU39097_at, VIT_04s0079g00680), for a zeaxanthin epoxidase (VVTU6355_at, VIT_07s0031g00620) and for a Beta-carotene hydroxylase (VVTU13738_at, VIT_16s0050g01090) are down-regulated at EL 36 vs EL 35 in all varieties. However, it is interesting to note that in Touriga Nacional we found up-regulation at EL 36 vs EL 35 of genes coding for a Zeta-carotene desaturase ZDS1 (VVTU4228_at, VIT_14s0030g01740) and a Beta-carotene hydroxylase (VVTU13791_at, VIT_02s0025g00240) involved in carotenoid biosynthesis as well as a gene coding for phytoene synthase (VVTU9210_a, VIT_13s0019g01270) that was up-regulated in Trincadeira.

Volatile terpenes may derive from the cleavage of carotenoids by carotenoid cleavage dioxygenases [56]. A gene coding for a *cis*-epoxycarotenoid dioxygenase 2 (isoenzyme carotenoid cleavage dioxygenase 1; VVTU8254_at, VIT_02s0087g00930) was up-regulated at EL36 vs EL 35 in Touriga Nacional whereas another (VVTU17555_s_at, VIT_10s0003g03750) was down-regulated in Trincadeira. Some flavor volatiles peak at pre-*véraison* or *véraison* stages and others at ripe or harvest stage and this may be also dependent on the variety. The volatiles (E)-2-Pentenal, 2-Ethylfuran, 2-Pentylfuran, (E, E)-2,4-Hexadien-1-al, 3-Methylbutanol, 3-Methylbutanal, benzaldehyde, 6-Methyl-5-hepten-2-one,

and (Z)-3-Octen-1-ol were higher at EL32 while (E)-2-Heptenal was more present at both pre-*véraison* or *véraison* stages.

The volatiles ethanol, hexanal, decanal and nonanal increased their content at ripe and harvest stages while (E)-2-Hexenal peaked at EL 36. The content in the putatively identified undecane peaked at EL 35 or EL 36 depending on the variety while heptanal at EL 36 and limonene at EL 38.

Carotenoid cleavage dioxygenases have been reported to generate 6-Methyl-5-hepten-2-one from lycopene [58]. This compound is an important flavor volatile in tomato [59] and tends to be higher in Trincadeira at EL 38 comparing to the other varieties. Different aroma profiles may also be related to the fact that a gene coding for myrcene synthase (VVTU36515_at, VIT_00s0271g00030) was down-regulated at EL 36 vs EL 35 in Trincadeira and Aragonês but not in Touriga Nacional.

Terpenes which are precursors for important aroma compounds start to accumulate at *véraison* [60]. A gene coding for a (-)-isopiperitenol dehydrogenase (VVTU2626_at, VIT_17s0000g05580) putatively involved in monoterpene biosynthesis was up-regulated at EL 36 vs EL 35 but only in Touriga Nacional. On the other hand, a gene coding for (+)-neomenthol dehydrogenase (VVTU7133_s_at, VIT_15s0046g03570) putatively involved in menthol biosynthesis, a volatile monoterpene, was down-regulated in all the varieties but another one (VVTU21725_at, VIT_15s0046g03600) was up-regulated at EL 36 vs EL 35 only Touriga Nacional and Aragonês. From the above it is not surprising that wines made from Touriga Nacional berries are recognized as being highly aromatic.

Furthermore, the putatively identified cyclic terpene limonene that provides a lemon-like fresh aroma reached the highest concentrations at harvest stage (EL 38) in Trincadeira and in particular in Touriga Nacional. In fact, Touriga Nacional wines are known to have an aroma of orange tree flower. Higher-quality Touriga Nacional wines are characterized by a fruity-citric aroma described as sweet and fresh citrus evoking the bergamot fruit (*Citrus bergamia*) [61]. In accordance, we have noticed in Touriga Nacional and by real time qPCR a very significant increase at EL 38 (Fig.7) in the expression of a gene coding for a terpene synthase which previous functional characterization showed that produces mainly (E)-a-bergamotene (VvTPS10; [62]). On the other hand, a terpene synthase that produces mainly (E)-b-ocimene (VvTPS34,[62]) was up-regulated at EL 38 in all the varieties but mainly in Aragonês highlighting aroma cultivar specificities.

We have observed down-regulation at EL 36 vs EL 35 of a gene coding for a limonoid UDP-glucosyltransferase in all varieties (VVTU17111_s_at, VIT_03s0180g00200 Table 2) putatively involved in limonoid glucoside synthesis from limonin [63]. In particular in Aragonês a considerable decrease in expression was noticed from EL 32 to EL 35 as shown by RT qPCR (Fig. 7). Limonoids are highly oxygenated triterpenes and one of the components responsible for the bitterness in citrus fruit [63]. The lower synthesis of their glucosides may be related to increased citric aroma. This gene was also shown to be induced during early withering in grape [64].

One gene coding for a lactoylglutathione lyase (VVTU11834_at, VIT_09s0002g06420) was up-regulated whereas another one (VVTU9837_s_at, VIT_04s0008g03560) was down-regulated EL 36 vs EL 35 in all varieties. The same holds true for four genes coding for aldo-keto reductase (VVTU4697_at, VIT_08s0007g01040, VVTU9888_at, VIT_05s0049g01130, VVTU11927_at, VIT_05s0062g00980, VVTU3533_s_at, VIT_05s0077g01300). Lactoylglutathione lyase or glyoxalase I is involved in the detoxification of methylglyoxal together with aldo-keto reductase. Dicarbonyl compounds, like methylglyoxal, are

often associated with amino acids in the formation of odorous products present in wine so the previously mentioned enzymes may play a role in wine aroma. For instance, leucine and methylglyoxal give rise to 3-methylbutanal responsible for a moderate amylic aroma [65]. This compound reached the highest values in Touriga Nacional at harvest stage.

Among other important volatiles is the alcohol 3-methylbutanol considered as a key-odorant in Grenache, Cabernet Sauvignon and Merlot wines [66]. This compound was presented in higher concentration in Touriga Nacional and Aragonês berries at EL 32 but decreased during ripening in both varieties showing no significant differences from Trincadeira at EL 38. Benzaldehyde also decreased at EL 36 and EL 38. Therefore these compounds cannot be used to discriminate the potential aroma of wines made from these varieties.

Benzoic acid which may constitute a precursor of volatile benzenoids [67] also showed a tendency to decrease in all varieties during ripening.

The majority of cyanogenic glucosides are derivatives of benzaldehyde cyanohydrin (mandelonitrile, i.e. nitrile of mandelic acid). Cyanogenic glycosides may be defined chemically as glycosides of α -hydroxynitriles and function in nitrogen storage for germination and plantlet development, and pathogen and herbivory defense [68]. The involvement of cyanogenic glycosides in fruit ripening has been previously mentioned for strawberry [69]. In grapevine, cyanogenesis (release of cyanide) has been detected in leaves but not in berries though the possibility that cyanogenic compounds, are present in berries remains to be excluded [70]. Interestingly, a gene coding for beta-cyanoalanine synthase (VVTU13018_s_at, VIT_15s0046g02300) putatively involved in cyanide detoxification was up-regulated at EL 36 vs EL 35 but only in Aragonês.

Among other free volatiles reported in grapes are C6 alcohols and aldehydes derived from linoleate cascade through activity of lipoxygenases [71].

We have observed up-regulation of an enzyme coding for a lipoxygenase (VVTU13955_at, VIT_14s0128g00780) that was up-regulated at EL 36 vs EL 35 but only in Touriga Nacional and Trincadeira. Since these varieties present more (E)-2-Hexenal and hexanal especially at EL 36 we can speculate whether the gene coding for this enzyme is involved in the synthesis of these C6 aldehydes. Previously and in Cabernet Sauvignon grapes, both (E)-2-hexenal and hexanal showed a significant increase after *veraison* followed by a decrease in the harvest sample [72]. It is also interesting to note that a gene coding for fatty acid hydroperoxide lyase (HPL1; VVTU37595_s_at, VIT_12s0059g01060) was down-regulated at EL36 vs EL 35 but only in Aragonês. Hexenal can be converted to hexanol by alcohol dehydrogenases. One gene coding for alcohol dehydrogenase was up-regulated at EL 36 vs EL 35 (VVTU4210_at, VIT_14s0068g01760) in all varieties. Production of volatiles as a result of alcohol dehydrogenase activity was suggested to contribute to the development of taste and aroma in fruits [73].

Besides hexenal and (E)-2-hexenal other aliphatic aldehydes such as octanal and (E)-2-heptenal provide an herbaceous odor. Octanal seems to be in higher amounts in Trincadeira at EL 38 whereas (E)-2-heptenal is present at EL 35.

(E)-2-heptenal or *trans*-2-heptenal, and (E)-2-hexenal or *Trans*-2-hexenal are known to provide fruity, green, leafy notes [74]. Decanal is associated with citrus peel and “sawdust” or “plant” odor [75] and accumulate in Trincadeira at EL 36 and EL 38. Nonanal with a fatty-green aroma [76] also accumulates at these stages in particular in this variety.

Genes coding for carboxylesterases were up or down-regulated at EL 36 vs EL 35 in only some varieties (File S3). These enzymes are involved in hydrolysis of esters into acids and alcohols and may contribute to flavor development.

Interestingly, anthraniloyl-CoA: methanol anthraniloyl transferase putatively involved in the biosynthesis of fruit esters responsible for aroma was up-regulated from EL 35 to EL 36 vs EL 35 in all varieties (VVTU5363_at, VIT_09s0018g01490). It is difficult to establish the activity of the enzyme coded by this gene since it shows strong homology with other acyltransferases responsible for synthesis of flavor compounds but it may be involved in the synthesis of the volatile methyl anthranilate [77].

S-adenosyl-L-methionine-dependent methyltransferases catalyze methylation of several molecules, and are key enzymes in phenylpropanoid, flavonoid and many other metabolic pathways. Enzymatic methylation of hydroxyl and carboxyl moieties is catalyzed by O-methyltransferases which include SAM: salicylic acid carboxy methyltransferases, SAM: jasmonic acid carboxyl methyltransferases and SAM: benzoic acid carboxyl methyltransferases, among others [78]. A gene coding for a S-adenosyl-L-methionine:salicylic acid carboxyl methyltransferase (VVTU5372_s_at, VIT_04s0023g02280) was down-regulated at EL36 vs EL 35, and may play an important role in specific aroma production at earlier stages of berry development [78]. Other two genes, however, were expressed either in Touriga Nacional (VVTU14878_s_at, VIT_04s0023g02200) or in Aragonês and Trincadeira (VVTU8882_at, VIT_01s0011g05920). A gene coding for a caffeic acid methyltransferase (VVTU36927_x_at, VIT_12s0059g01790) putatively involved in aroma production was also down-regulated at EL 36 vs EL 35 as it was already referred for a decrease in the compound caffeic acid. RT qPCR data showed that this gene presented a major decrease from EL 32 to EL 35 in particular in Aragonês cultivar (Fig. 7).

Other methyltransferases such as O-methyltransferases may be involved in the synthesis of vanillin [79] which precursor is vanillic acid. The presence of this compound was only identified in grapes at EL 36 and EL 38 stages of ripening and shown to be present at higher amounts in Touriga Nacional, highlighting the known aromatic potential of these grapes. In fact, ethyl vanillate was shown to be present in clonal red wines from Touriga Nacional (Falco da Costa, personal communication). It should be pointed out that methyltransferases constitute a protein family in which little correlation is observed between the level of sequence similarity among enzymes and the structural similarity of their substrates so their activities should be discussed with caution [56]. Cytochrome P450 are also involved in the formation of plant volatiles and in a vast array of biosynthetic pathways in secondary and primary metabolism [56]. A gene coding a CYP89H3 (VVTU21329_at, VIT_16s0039g00880) was up-regulated at EL 36 vs EL 35 in all varieties in particular in Trincadeira while the expression values at EL 38 were similar among the varieties (Fig. 7). Other genes coding for CYPs were up-regulated in one or two varieties and may eventually be involved in aroma development (File S3).

It was noticed the up-regulation of a gene coding for alliin lyase precursor (VVTU16622_at, VIT_00s0225g00230) in all varieties, especially in Trincadeira. Alliin lyase (alliinase) gives rise to volatile sulphur compounds from S-alk(en)yl cysteine sulphoxide flavor precursors derived from cysteine and glutathione [80]. This latter compound was shown to increase during ripening of Trincadeira grapes [11]. Moreover, glutathione and *trans*-2-hexenal intervene in the biosynthesis of S-(3-hexan-1-ol)-glutathione which is a flavor precursor in wines [81]. In fact, most of the volatile sulphur compounds that contribute to varietal character are released

during must fermentation from specific aroma/flavor precursors present in the grapes [82].

The varietal aroma is built on different classes of compounds that may be more present in one variety independently of the *terroir*. Nevertheless at *veraison* aromas and flavors begin to develop in all varieties and increase their complexity during ripening. For all the varieties studied pre-*veraison* and *veraison* stages seem to be enriched in carotenoids, benzaldehyde and caffeic acid and post-*veraison* stages in volatile terpenes and sulfur compounds, C6 alcohols and aldehydes, and vanillic acid.

Conclusions

This work performed a comprehensive analysis and interpretation of the transcriptome and metabolome of pre-ripe and ripe grapes of three Portuguese cultivars. The combined analysis of transcripts and metabolites contributed to the establishment of putative markers of pre-ripening and ripening involved in carbohydrate, lipid, amino acid and phenylpropanoid metabolisms (Fig. 9). The decrease in metabolites of the TCA cycle during ripening may be due to their use for increased amino acid biosynthesis as previously revealed by NMR studies with the exception being glutamate [11]. On the other hand, shikimate synthesized from the precursor phosphoenolpyruvate may be consumed for the synthesis of phenolics whereas pyruvate is likely to be used for fatty acid biosynthesis, branched chain aminoacids and isoprenoids.

Good correlations were found for the content of campesterol and the genes coding for enzymes involved in steroid biosynthesis. The same holds true for sucrose and a gene coding for sucrose phosphatase; for ascorbate and a gene coding for L-Galactono-1,4-lactone dehydrogenase; for glycolic acid and a gene coding for glyoxalate reductase; for resveratrol and genes coding for stilbenes synthase, among others. We have also validated a previous identified biomarker of pre-ripe berries which is a gene coding for 11- β -hydroxysteroid dehydrogenase. These biomarkers can be

further validated in the future for other cultivars and over different seasons to exclude any potential climate or *terroir* effect. The candidate molecular biomarkers presented here were already validated for Trincadeira during 2007 season (GEO accession number GSE28779).

On the other hand, the use of approaches enabling both gene expression and metabolites content gave strong insights into how aroma is developed during ripening, and also in to those features which are cultivar specific. The differential accumulation of organic acids among the three varieties may result in a different pool of phenolic compounds and amino acids. In addition, several genes coding for enzymes of either the phenylpropanoid or the terpenoid pathway were differently expressed among the three varieties and may reflect the different content in volatiles. On the other hand, this differential gene expression may lead to the synthesis of glycosides with aromatic potential that were not addressed in this work but certainly deserve attention.

Altogether the data discussed here contributed for a better understanding of the metabolic pathways involved in berry ripening through establishment of candidate molecular and metabolic markers that may define key switches in cellular reprogramming. It was also a contribution for the understanding of the complex process of flavor development that characterizes a specific variety.

Materials and Methods

Sample collection

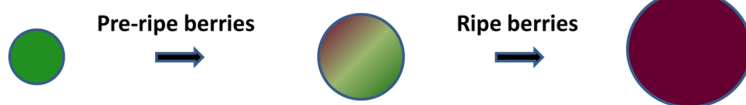
Four biological replicates (each including 80–100 berries from 8–10 plants) were collected around 10 a.m. in 2008 at Plansels vines located in Montemor-o-Novo (Southern Portugal). The sampling was carried out with permission from the owner of Plansel, a private company. Samples from three important Portuguese cultivars (Aragonês, Touriga Nacional and Trincadeira, Figure S1) corresponding to the developmental stages of EL 32, 35, 36, and 38 (EL refers to the modified Eichhorn and Lorenz

Accumulation of metabolites:

Organic acids (glycerate, glycolate, malate, tartaric acid, ascorbate), campesterol, glycerol 3-phosphate, shikimate, quercetin, catechin, gallic acid, caffeic acid, *p*-coumaric acid, (E)-2-Heptenal

Accumulation of metabolites:

Glucose, fructose, dehydroascorbic acid, β -sedoheptulose, saturated fatty acids, tocopherol, ampelopsin, resveratrol, ethanol, decanal, nonanal hexanal, (E)-2-Hexenal, limonene, vanillic acid



Expression of genes coding for:

vacuolar invertases, L-Galactono-1,4-lactone dehydrogenase, cytosolic fructose-1,6-bisphosphatase, tonoplast dicarboxylate transporter, succinic semialdehyde dehydrogenase, glyoxylate reductase, FAD6, FAD3, squalene synthase, 11- β -hydroxysteroid dehydrogenase, glutamate dehydrogenase 1, zeaxanthin epoxidase, limonoid UDP-glucosyltransferase, caffeic acid O-methyltransferase

Expression of genes coding for:

Sucrose phosphatase, Galactinol synthase, cytosolic pyruvate kinase, starch synthase, ATP-citrate synthase, 6-phosphogluconolactonase, FAB2, chloroplastidial palmitoyl-monogalactosyldiacylglycerol delta-7 desaturase, diacylglycerol kinase, 1-acyl-sn-glycerol-3-phosphate acyltransferase, trans-cinnamate 4-monooxygenase, stilbene synthase, anthraniloyl-CoA: methanol anthraniloyl transferase, CYP89H3

Figure 9. Candidate molecular and metabolic markers of pre-ripe and ripe berries established in three Portuguese varieties.
doi:10.1371/journal.pone.0060422.g009

developmental scale as described by [4]) were immediately frozen in liquid nitrogen, transported to the lab in dry ice and kept at -80°C . Each biological replicate contained berries from a single row of plants, and from the sunny and shady sides of the plants that were pooled to form mixed samples. Rows distant 3 to 10 m were used. Plants from the three varieties were growing in the vineyard 15–30 m apart (Figure S2). The experiments were conducted on healthy grapes presenting no visible signs of fungal attack or other microbiological alteration. Meteorological conditions are shown in File S4.

RNA extraction

RNA extraction from pulp and skin of berries was carried out as previously described [11]. A DNase treatment was performed according to the suppliers' instructions (Invitrogen, San Diego, CA, USA). Samples were then extracted in phenol/chloroform/isoamylalcohol (75:24:1,v/v/v), precipitated with sodium acetate and ethanol, washed in 70% ethanol and dissolved in water. RNA was further purified using RNeasy Plant Mini kit (Quiagen, Valencia, CA, USA).

Target preparation and hybridization of oligo arrays

RNA quality was checked using the Agilent 2100 Bioanalyzer (Agilent technologies, Palo Alto, CA). cDNA was synthesized from 4 μg of total RNA using One-cycle target labeling and control reagents (Affymetrix, Santa Clara, CA) to produce biotin labeled cRNA which was then fragmented at 94°C for 35 min into 35–200 bases in length.

Three biological replicates were independently hybridized to the GrapeGena 520510F array (Affymetrix, Santa Clara, CA). Each sample was added to a hybridization solution containing 100 mM 2-(N-morpholino) ethanesulfonic acid, 1 M NaCl, and 20 mM of EDTA in the presence of 0.01% of Tween-20 to a final cRNA concentration of 0.05 $\mu\text{g}/\text{ml}$. Hybridization was performed for 16 h at 45°C . Each microarray was washed and stained with streptavidin-phycoerythrin in a Fluidics station 450 (Affymetrix) and scanned at 1.56 μm resolution in a GeneChip[®] Scanner 3000 7G System (Affymetrix).

Data and sequences analysis and gene annotation

Robust Multi-array Analysis (RMA) algorithm was used for background correction, normalization and expression levels summarization [83]. Next, differential expression analysis was performed with the Bayes t-statistics from the linear models for Microarray data (limma), included in the affyGUI package. P-values were corrected for multiple-testing using the Benjamini-Hochberg's method [14]. Data obtained from hybridization of GrapeGen chips was filtered considering a fold change ≥ 1.5 and corrected p value < 0.05 or fold change ≤ -1.5 and a corrected p value < 0.05 .

The probesets sequences were blasted against the genes predicted from the genome (blastn, e-value $< e^{-20}$, minimum of 100 bp alignment) available at the NCBI website. Gene annotation was performed by updating the annotation performed in [84] following the same protocol as described by the authors to the new genes from the 12 \times coverage release of the genome assembly.

The microarray data were submitted to Gene Expression Omnibus (NCBI), and are accessible through GEO accession number GSE35172.

Anthocyanins quantification

Fifty-one hundred milligrams of lyophilized material and 50% methanol were mixed to get a final suspension of 50 mg/mL (w/

v). Two volumes of acidic methanol (1% HCl in 50% MeOH) were added and absorption read at 530 nm using quartz microcuvettes. Total relative anthocyanin concentration was expressed as the absorbance value at 530 nm/g of freeze-dried weight.

Quantitative RT-PCR

Complementary DNA was synthesized from 1.5 μg RNA using a RevertAid[™] H Minus M-MuLV Reverse Transcriptase (Fermentas, Burlington, Canada) according to the manufacturer's instructions. Primers sequences (Table S1) were selected using Primer express software3.0 (Applied Biosystems, Foster City, CA). Real-time PCR reactions were prepared using Maxima[™] SYBR Green qPCR Master Mix (2 \times) (Fermentas, Burlington, Canada) and performed using the StepOne[™] Real-Time PCR System (Applied Biosystems, Foster City, CA). Cycling conditions were 95°C for 20 min, then 40 cycles of 95°C for 1 min and 60°C for 20 min. Expression was determined for duplicate biological replicates and triplicate technical replicates using a serial dilution cDNA standard curve per gene. Data were calculated from the calibration curve and normalized using the expression curve of actin gene (VVTU17999_s_at) that presented absolutely no differential expression in the microarray analysis.

Soluble Metabolites

The profiling of soluble metabolites was performed as detailed previously [85,86]; by gas chromatography coupled to electron impact ionization/time-of-flight mass spectrometry (GC-EI/TOF-MS) using an Agilent 6890N24 gas chromatograph (Agilent Technologies, Böblingen, Germany; <http://www.agilent.com>) with splitless injection onto a FactorFour VF-5 ms capillary column, 30-m length, 0.25-mm inner diameter, 0.25- μm film thickness (Varian-Agilent Technologies), which was connected to a Pegasus III time-of-flight mass spectrometer (LECO Instrumente GmbH, Mönchengladbach, Germany; <http://www.leco.de>).

Soluble metabolites were extracted from 300 mg (fresh weight $\pm 10\%$ tolerance) deep frozen powder by 1 mL ethylacetate with 2 h agitation at 30°C . Aliquots of 300 μL from the ethylacetate fraction were dried by vacuum concentration and stored dry under inert gas at -20°C until further processing. Metabolites were methoxyaminated and trimethylsilylated manually prior to GC-EI/TOF-MS analysis [86]. Retention indices were calibrated by addition of a C₁₀, C₁₂, C₁₅, C₁₈, C₁₉, C₂₂, C₂₈, C₃₂, and C₃₆ n-alkane mixture to each sample [87].

GC-EI/TOF-MS chromatograms were acquired, visually controlled, baseline corrected and exported in NetCDF file format using ChromaTOF software (Version 4.22; LECO, St. Joseph, USA). GC-MS data processing into a standardized numerical data matrix and compound identification were performed using the TagFinder software [88,89]. Compounds were identified by mass spectral and retention time index matching to the reference collection of the Golm metabolome database (GMD, <http://gmd.mpimpgolm.mpg.de/>; [90,91]). Guidelines for manually supervised metabolite identification were the presence of at least 3 specific mass fragments per compound and a retention index deviation $< 1.0\%$ [87]. All mass features of an experiment were normalized by sample fresh weight, internal standard (C₂₂) and maximum scaled.

Volatile Metabolites

The profiling of volatile metabolites was performed using 1 g (fresh weight $\pm 10\%$ tolerance) of deep frozen powder which was suspended in 1 mL H₂O and 0.2 g NaCl using 20 mL head-space-vials (Gerstel, Mülheim an der Ruhr, Germany). Analyses were performed by solid phase micro extraction (SPME) and gas

chromatography coupled to electron impact ionization/quadrupole mass spectrometry (GC-EI-MS) using an Agilent 6890N24 gas chromatograph (Agilent Technologies, Böblingen, Germany; <http://www.agilent.com>) and a StableFlex™ SPME-fiber with 65 µm polydimethylsiloxane/divinylbenzene (PDMS-DVB) coating (Supelco, Bellefonte, USA). SPME samples were taken from the headspace with 10 min incubation at 45°C, 5 min adsorption at 45°C and 1 min desorption at 250°C onto a DB-624 capillary column with 60-m length, 0.25-mm inner diameter, 1.40- µm film thickness (Agilent Technologies, Böblingen, Germany). The GC temperature programming was 2 min isothermal at 40°C followed by a 10°C/min ramping to 260°C final temperature which was held constant for 10 min. The Agilent 5975B VL GC-MSD system was operated with a constant flow of helium at 1.0 mL/min. Desorption from the SPME fiber was at 16.6 psi with an initial 0.1 min pulsed-pressure at 25 psi. The subsequent purge was 1 min at a purge flow of 12.4 mL/min. System stability was controlled and the sample sequence randomized. GC-EI-MS chromatograms were acquired with mass range set to 30–300 m/z and a 20 Hz scan rate. Chromatography data files were visually controlled, exported in NetCDF file format using Agilent ChemStation-Software and baseline-corrected with MetAlign software [92]. GC-MS data processing into a standardized numerical data matrix and compound identification were performed as was described above using the TagFinder software [88,89]. Compounds were identified by mass spectral and retention time matching to the reference collection of the Golm Library for volatile compounds. Guidelines for manually supervised metabolite identification were the presence of at least 3 specific mass fragments per compound and a retention time deviation <3.0%. All mass features of an experiment were normalized by maximum scaling.

Relative Quantification of metabolite concentrations

For quantification purposes all mass features were evaluated for best specific, selective and quantitative representation of observed analytes. Laboratory and reagent contaminations were evaluated by non-sample control experiments. Metabolites were routinely assessed by relative changes expressed as response ratios, i.e. x-fold factors in comparison to a control condition or in comparison to the overall median of each metabolite measure.

Statistical analyses and data visualization

Statistical testing was performed using \log_{10} -transformed response ratios. Statistical assessments and heat map were performed with the multi-experiment viewer software, MeV (Version 4.6.2; <http://www.tm4.org/mev/>; [93] or the Microsoft-Excel 2007 program. Independent component analysis (ICA) of the first 5 principal components were performed using \log_{10} -

transformed response ratios via the MetaGeneAlyse web application (Version 1.7.1; <http://metagenealyse.mpimp-golm.mpg.de>) with missing value substitution, $\log_{10} = 0$. Excel files containing ion peak responses were used for Kruskal-Wallis and Wilcoxon rank sum tests in order to determine which samples have significantly different amounts of certain metabolites. For multiple comparisons the Benjamini & Hochberg correction was used which defines a sequential p-value procedure that controls the expected proportion of falsely rejected hypotheses - the false discovery rate (FDR). The FDR is a less stringent condition than the family-wise error rate (FWER), so this method is among the most powerful procedures for multiple testing.

Supporting Information

Figure S1 Samples of berries at EL 38 stage of development. A Aragonés B Touriga Nacional C Trincadeira. (PPTX)

Figure S2 Sketch of the sampling layout. (PPTX)

Table S1 List of primers used in real time reverse transcription-polymerase chain reaction. (DOCX)

File S1 List of volatiles and polar metabolites analyzed during grape ripening of the three cultivars under study. (XLSX)

File S2 Kruskal-Wallis and Wilcoxon Rank sum statistics applied to metabolomics data. For selected multiple comparisons the Benjamini & Hochberg correction was elected among other tests that are presented. (XLSX)

File S3 List of entire gene set (8696 probesets) and common gene set (2255 probesets) of modulated genes during grape ripening. Information concerning fold change values, annotation and functional category is provided. (XLSX)

File S4 Weather conditions from April to September in 2008 season. (XLSX)

Author Contributions

Conceived and designed the experiments: AMF JK. Performed the experiments: PAR AE AMF. Analyzed the data: PAR AE LS AMF. Contributed reagents/materials/analysis tools: MSP JK AMF. Wrote the paper: AMF JK.

References

1. Yadav M, Jain S, Bhardwaj A, Nagpal R, Puniya M, et al. (2009) Biological and medicinal properties of grapes and their bioactive constituents: an update. *J Med Food* 12: 473-484.
2. Ali K, Maltese F, Choi YH, Verpoorte R (2010) Metabolic constituents of grapevine and grape-derived products. *Phytochem Rev* 9: 357-378.
3. Coombe B, McCarthy M (2000) Dynamics of grape berry growth and physiology of ripening. *Australian Journal of Grape and Wine Research* 6: 131-135.
4. Coombe B (1995) Growth Stages of the Grapevine: Adoption of a system for identifying grapevine growth stages. *Australian Journal of Grape and Wine Research* 1: 104-110.
5. Terrier N, Glissant D, Grimplet J, Barrieu F, Abbal P, et al. (2005) Isogene specific oligo arrays reveal multifaceted changes in gene expression during grape berry (*Vitis vinifera* L.) development. *Planta* 222: 832-847.
6. Deluc LG, Grimplet J, Wheatley MD, Tillett RL, Quilici DR, et al. (2007) Transcriptomic and metabolite analyses of Cabernet Sauvignon grape berry development. *BMC Genomics* 8: 429.
7. Pilati S, Perazzolli M, Malossini A, Cestaro A, Demattè L, et al. (2007) Genome-wide transcriptional analysis of grapevine berry ripening reveals a set of genes similarly modulated during three seasons and the occurrence of an oxidative burst at véraison. *BMC Genomics* 8: 428.
8. Negri AS, Prinsi B, Rossoni M, Failla O, Scienza A, et al. (2008) Proteome changes in the skin of the grape cultivar Barbera among different stages of ripening. *BMC Genomics* 9: 378.
9. Zamboni A, Di Carli M, Guzzo F, Stocchero M, Zenoni S, et al. (2010) Identification of Putative Stage-Specific Grapevine Berry Biomarkers and Omics Data Integration into Networks. *Plant Physiology*: 1439-1459.
10. Martínez-Esteso MJ, Sellés-Marchart S, Lijavetzky D, Pedreño MA, Bru-Martínez R (2011) A DIGE-based quantitative proteomic analysis of grape berry

- flesh development and ripening reveals key events in sugar and organic acid metabolism. *J Exp Bot* 62: 2521-2569.
11. Fortes AM, Agudelo-Romero P, Silva MS, Ali K, Sousa L, et al. (2011) Transcript and metabolite analysis in Trincadeira cultivar reveals novel information regarding the dynamics of grape ripening. *BMC Plant Biol* 11: 149.
 12. Ali MB, Howard S, Chen S, Wang Y, Yu O, et al. (2011) Berry skin development in Norton grape: distinct patterns of transcriptional regulation and flavonoid biosynthesis. *BMC Plant Biol* 11: 7.
 13. Ali K, Maltese F, Fortes A, Pais M, Choi Y, et al. (2011) Monitoring biochemical changes during grape berry development in Portuguese cultivars by NMR spectroscopy. *Food Chemistry*: 1760-1769.
 14. Benjamini Y, Hochberg Y (1995) Controlling the false discovery rate: A practical and powerful approach to multiple testing. *Journal of the Royal Statistical Society Series B (Methodological)* 57: 289-300.
 15. Vignault C, Vachaud M, Cakir B, Glissant D, Dédaldéchamp F, et al. (2005) VvHT1 encodes a monosaccharide transporter expressed in the conducting complex of the grape berry phloem. *J Exp Bot* 56: 1409-1418.
 16. Zhang XY, Wang XL, Wang XF, Xia GH, Pan QH, et al. (2006) A shift of Phloem unloading from symplasmic to apoplasmic pathway is involved in developmental onset of ripening in grape berry. *Plant Physiol* 142: 220-232.
 17. Dai ZW, León C, Feil R, Lunn JE, Delrot S, et al. (2013) Metabolic profiling reveals coordinated switches in primary carbohydrate metabolism in grape berry (*Vitis vinifera* L.), a non-climacteric fleshy fruit. *J Exp Bot*.
 18. Davies C, Wolf T, Robinson S (1999) Three putative sucrose transporters are differentially expressed in grapevine tissues. *Plant Science*: 93-100.
 19. Takashima Y, Senoura T, Yoshizaki T, Hamada S, Ito H, et al. (2007) Differential chain-length specificities of two isomylase-type starch-debranching enzymes from developing seeds of kidney bean. *Biosci Biotechnol Biochem* 71: 2308-2312.
 20. Janssen B, Thodey K, Schaffer R, Alba R, Balakrishnan L, et al. (2008) Global gene expression analysis of apple fruit development from the floral bud to ripe fruit. *Bmc Plant Biology*: -.
 21. Conde C, Delrot S, Geros H (2008) Physiological, biochemical and molecular changes occurring during olive development and ripening. *Journal of Plant Physiology*: 1545-1562.
 22. Grant T, Dami I, Ji T, Scurlock D, Streeter J (2009) Variation in leaf and bud soluble sugar concentration among *Vitis* genotypes grown under two temperature regimes. *Canadian Journal of Plant Science* 89: 961-968.
 23. Sweetman C, Deluc LG, Cramer GR, Ford CM, Soole KL (2009) Regulation of malate metabolism in grape berry and other developing fruits. *Phytochemistry* 70: 1329-1344.
 24. Livio T, Tadiello A, Casadoro G (2007) Variations of the peach fruit transcriptome during ripening and in response to hormone treatments. *Caryologia*: 156-159.
 25. Mellema S, Eichenberger W, Rawlyer A, Suter M, Tadege M, et al. (2002) The ethanolic fermentation pathway supports respiration and lipid biosynthesis in tobacco pollen. *Plant J* 30: 329-336.
 26. Wills R, Wimalasiri P, Greenfield H (1984) Dehydroascorbic acid levels in fresh fruit and vegetables in relation to total vitamin-C activity. *Journal of Agricultural and Food Chemistry*: 836-838.
 27. Okuda T, Yokotsuka K (1999) Levels of glutathione and activities of related enzymes during ripening of koshiu and Cabernet Sauvignon grapes and during winemaking. *American Journal of Enology and Viticulture*: 264-270.
 28. Helsper J, Loeuw F (1982) Metabolism of L-threonine acid in *Rumex-x-acutus* L and *Pelargonium crispum* (L) Lher. *Plant Physiology*: 1365-1368.
 29. Millán C, Vargas A, Rubio A, Moreno J, Ortega J (1992) Fatty acid content of unripe and ripe 'Pedro Ximénez' *Vitis vinifera* grapes. *Journal of Wine Research* 3.
 30. Grncarevic M, Radler F (1971) A Review of the Surface Lipids of Grapes and Their Importance in the Drying Process. *Am J Enol Vitic* 22: 80-86.
 31. Commenil P, Brunet L, Audran J (1997) The development of the grape berry cuticle in relation to susceptibility to bunch rot disease. *Journal of Experimental Botany*: 1599-1607.
 32. Zhang J, Wang X, Yu O, Tang J, Gu X, et al. (2011) Metabolic profiling of strawberry (*Fragaria xananassa* Duch.) during fruit development and maturation. *Journal of Experimental Botany*: 1103-1118.
 33. Byfield G, Upchurch R (2007) Effect of temperature on delta-9 stearoyl-ACP and microsomal omega-6 desaturase gene expression and fatty acid content in developing soybean seeds. *Crop Science*: 1698-1704.
 34. Liu Z, Yang X, Fu Y (2009) SAD, a Stearoyl-Acyl Carrier Protein Desaturase Highly Expressed in High-Oil Maize Inbred Lines. *Russian Journal of Plant Physiology*: 709-715.
 35. Whitaker B, Gapper N (2008) Ripening-specific stigmaterol increase in tomato fruit is associated with increased sterol C-22 desaturase (CYP710A11) gene expression. *Journal of Agricultural and Food Chemistry*: 3828-3835.
 36. Chow E, Jen J (1978) Phytosterol biosynthesis in ripening tomatoes. *Journal of Food Science*: 1424-1426.
 37. Symons G, Davies C, Shavruk Y, Dry I, Reid J, et al. (2006) Grapes on steroids. Brassinosteroids are involved in grape berry ripening. *Plant Physiology*: 150-158.
 38. Karlova R, Rosin F, Busscher-Lange J, Parapunova V, Do P, et al. (2011) Transcriptome and Metabolite Profiling Show That APETALA2a Is a Major Regulator of Tomato Fruit Ripening. *Plant Cell*: 923-941.
 39. Lung SC, Weselake RJ (2006) Diacylglycerol acyltransferase: a key mediator of plant triacylglycerol synthesis. *Lipids* 41: 1073-1088.
 40. Bianchi G, Murelli C, Vlahov G (1992) Surface waxes from olive fruits. *Phytochemistry*: 3503-3506.
 41. Saber M, Kashmiri M, Mohy-Ud-Din A, Ahmad M, Khanum R (2010) Epicuticular Wax of *Tamarix aphylla* L. *Journal of the Chemical Society of Pakistan*: 662-667.
 42. Arisz S, Testerink C, Munnik T (2009) Plant PA signaling via diacylglycerol kinase. *Biochimica Et Biophysica Acta-Molecular and Cell Biology of Lipids*: 869-875.
 43. Camara B, Brangeon J (1981) Carotenoid metabolism during chloroplast to chromoplast transformation in *Capsicum annum* fruit. *Planta*: 359-364.
 44. Jackson RS (2000) Wine science: principles and applications: Elsevier.
 45. van Damme M, Zeilmaker T, Elberse J, Andel A, de Sain-van der Velden M, et al. (2009) Downy Mildew Resistance in Arabidopsis by Mutation of HOMOSERINE KINASE. *Plant Cell*: 2179-2189.
 46. Agudelo-Romero P, Bortolotti C, Pais MS, Tiburcio A, Fortes AM (2013) Study of Polyamines during Grape Ripening Indicate an Important Role of Polyamine Catabolism. *Plant Physiology and Biochemistry* accepted.
 47. Downey M, Harvey J, Robinson S (2003) Synthesis of flavonols and expression of flavonol synthase genes in the developing grape berries of Shiraz and Chardonnay (*Vitis vinifera* L.). *Australian Journal of Grape and Wine Research* 9: 110-121.
 48. Zheng HQ, Liu DY (2003) [Anti-invasive and anti-metastatic effect of amepolisin on melanoma]. *Ai Zheng* 22: 363-367.
 49. Harbertson J, Kennedy J, Adams D (2002) Tannin in skins and seeds of Cabernet Sauvignon, Syrah, and Pinot noir berries during ripening. *American Journal of Enology and Viticulture*: 54-59.
 50. Katiyar SK, Afaq F, Perez A, Mukhtar H (2001) Green tea polyphenol (-)-epigallocatechin-3-gallate treatment of human skin inhibits ultraviolet radiation-induced oxidative stress. *Carcinogenesis* 22: 287-294.
 51. Toffali K, Zamboni A, Anesi A, Stocchero M, Pezzotti M, et al. (2011) Novel aspects of grape berry ripening and post-harvest withering revealed by untargeted LC-ESI-MS metabolomics analysis. pp.424-436.
 52. Pereira D, Valentao P, Pereira J, Andrade P (2009) Phenolics: From Chemistry to Biology. *Molecules*: 2202-2211.
 53. Ali K, Iqbal M, Korthout H, Maltese F, Fortes A, et al. (2012) NMR spectroscopy and chemometrics as a tool for anti-TNF α activity screening in crude extracts of grapes and other berries. *Metabolomics*.
 54. Bogs J, Ebadi A, McDavid D, Robinson S (2006) Identification of the flavonoid hydroxylases from grapevine and their regulation during fruit development. *Plant Physiology*: 279-291.
 55. Croft K (1998) The chemistry and biological effects of flavonoids and phenolic acids: towards prolongation of the healthy life span. *Annals of the New York Academy of Sciences* 854: 435-442.
 56. Pichersky E, Noel J, Dudareva N (2006) Biosynthesis of plant volatiles: Nature's diversity and ingenuity. *Science*: 808-811.
 57. Oliveira C, Silva Ferreira AC, Mendes Pinto M, Hogg T, Alves F, et al. (2003) Carotenoid compounds in grapes and their relationship to plant water status. *J Agric Food Chem* 51: 5967-5971.
 58. Vogel J, Tan B, McCarty D, Klec H (2008) The carotenoid cleavage dioxygenase 1 enzyme has broad substrate specificity, cleaving multiple carotenoids at two different bond positions. *Journal of Biological Chemistry*: 11364-11373.
 59. Gao H, Zhu H, Shao Y, Chen A, Lu C, et al. (2008) Lycopene accumulation affects the biosynthesis of some carotenoid-related volatiles independent of ethylene in tomato. *J Integr Plant Biol* 50: 991-996.
 60. Lucker J, Bowen P, Bohlman J (2004) *Vitis vinifera* terpenoid cyclases: functional identification of two sesquiterpene synthase cDNAs encoding (+)-valencene synthase and (-)-germacrene D synthase and expression of mono- and sesquiterpene synthases in grapevine flowers and berries. *Phytochemistry* 65: 2649-2659.
 61. De Pinho PG, Falqué E, Castro M, Oliveira E Silva H, Machado B, et al. (2007) Further insights into the floral character of Touriga Nacional wines. *J Food Sci* 72: S396-401.
 62. Martin D, Aubourg S, Schouwey M, Daviet L, Schalk M, et al. (2010) Functional Annotation, Genome Organization and Phylogeny of the Grapevine (*Vitis vinifera*) Terpene Synthase Gene Family Based on Genome Assembly, FLeDNA Cloning, and Enzyme Assays. *Bmc Plant Biology* 10.
 63. Kita M, Hirata Y, Moriguchi T, Endo-Inagaki T, Matsumoto R, et al. (2000) Molecular cloning and characterization of a novel gene encoding limonoid UDP-glucosyltransferase in Citrus. *Febs Letters*: 173-178.
 64. Zamboni A, Minoia L, Ferrarini A, Tornielli G, Zago E, et al. (2008) Molecular analysis of post-harvest withering in grape by AFLP transcriptional profiling. *Journal of Experimental Botany*: 4145-4159.
 65. Pripis-Nicolau L, de Revel G, Bertrand A, Maujean A (2000) Formation of flavor components by the reaction of amino acid and carbonyl compounds in mild conditions. *Journal of Agricultural and Food Chemistry*: 3761-3766.
 66. Kotseridis Y, Baumes R (2000) Identification of impact odorants in Bordeaux red grape juice, in the commercial yeast used for its fermentation, and in the produced wine. *Journal of Agricultural and Food Chemistry*: 400-406.
 67. D'Auria J, Chen F, Pichersky E (2002) Characterization of an acyltransferase capable of synthesizing benzylbenzoate and other volatile esters in flowers and damaged leaves of *Clarkia breweri*. *Plant Physiology*: 466-476.

68. Vetter J (2000) Plant cyanogenic glycosides. *Toxicon* 38: 11-36.
69. Aharoni A, O'Connell A (2002) Microarray Gene Expression Analysis During Strawberry Achenes and Receptacle Maturation. *Journal of Experimental Botany* 53: 2073-2087.
70. Franks TK, Hayasaka Y, Choimes S, van Heeswijk R (2005) Cyanogenic glycosides in grapevine: polymorphism, identification and developmental patterns. *Phytochemistry* 66: 165-173.
71. Creelman R, Mullet J (1997) Biosynthesis and action of jasmonates in plants. *Annual Review of Plant Physiology and Plant Molecular Biology*: 355-381.
72. Kalua C, Boss P (2009) Evolution of Volatile Compounds during the Development of Cabernet Sauvignon Grapes (*Vitis vinifera* L.). *Journal of Agricultural and Food Chemistry*: 3818-3830.
73. Longhurst T, Tung H, Brady C (1990) Developmental regulation of the expression of alcohol dehydrogenase in ripening tomato fruit. *J Food Biochem* 14: 421-433.
74. Franco M, Peinado R, Medina M, Moreno J (2004) Off-vine grape drying effect on volatile compounds and aromatic series in must from Pedro Ximenez grape variety. *Journal of Agricultural and Food Chemistry*: 3905-3910.
75. Flamini R (2005) Some advances in the knowledge of grape, wine and distillates chemistry as achieved by mass spectrometry. *J Mass Spectrom* 40: 705-713.
76. Ong P, Acree T, Lavin E (1998) Characterization of volatiles in rambutan fruit (*Nephelium lappaceum* L.). *Journal of Agricultural and Food Chemistry*: 611-615.
77. Wang J, De Luca V (2005) The biosynthesis and regulation of biosynthesis of Concord grape fruit esters, including 'foxy' methylanthranilate. *Plant J* 44: 606-619.
78. Effmert U, Saschenbrecker S, Ross J, Negre F, Fraser C, et al. (2005) Floral benzenoid carboxyl methyltransferases: From in vitro to in planta function. *Phytochemistry*: 1211-1230.
79. Havkin-Frenkel D, Podstolski A, Witkowska E, Molecki P, Milkolajczyk M (1999) Vanillin biosynthetic pathways: an overview. In: T.J Fu, Singh G, Curtis WR, editors. *Plant Cell and Tissue Culture for the Production of Food Ingredients*. New York: Kluwer Academic Press/Plenum Publishers. pp. 35-43.
80. Jones M, Hughes J, Tregova A, Milne J, Tomsett A, et al. (2004) Biosynthesis of the flavour precursors of onion and garlic. *Journal of Experimental Botany*: 1903-1918.
81. Kobayashi H, Takase H, Suzuki Y, Tanzawa F, Takata R, et al. (2011) Environmental stress enhances biosynthesis of flavor precursors, S-3-(hexan-1-ol)-glutathione and S-3-(hexan-1-ol)-L-cysteine, in grapevine through glutathione S-transferase activation. *J Exp Bot* 62: 1325-1336.
82. Dubourdieu D, Torninaga T, Masneuf I, Des Gachons C, Murat M (2006) The role of yeasts in grape flavor development during fermentation: The example of Sauvignon blanc. *American Journal of Enology and Viticulture*: 81-88.
83. Irizarry R, Hobbs B, Collin F, Beazer-Barclay Y, Antonellis K, et al. (2003) Exploration, normalization, and summaries of high density oligonucleotide array probe level data. *Biostatistics*: 249-264.
84. Grimplet J, Cramer GR, Dickerson JA, Mathiason K, Van Hemert J, et al. (2009) VitisNet: "Omics" integration through grapevine molecular networks. *PLoS One* 4: e3365.
85. Wagner C, Sefkow M, Kopka J (2003) Construction and application of a mass spectral and retention time index database generated from plant GC/EI-TOF-MS metabolite profiles. *Phytochemistry*: 887-900.
86. Erban A, Schauer N, Fernie AR, Kopka J (2007) Nonsupervised construction and application of mass spectral and retention time index libraries from time-of-flight gas chromatography-mass spectrometry metabolite profiles. *Methods Mol Biol* 358: 19-38.
87. Strehmel N, Hummel J, Erban A, Strassburg K, Kopka J (2008) Retention index thresholds for compound matching in GC-MS metabolite profiling. *Journal of Chromatography B-Analytical Technologies in the Biomedical and Life Sciences*: 182-190.
88. Luedemann A, Strassburg K, Erban A, Kopka J (2008) TagFinder for the quantitative analysis of gas chromatography - mass spectrometry (GC-MS)-based metabolite profiling experiments. *Bioinformatics*: 732-737.
89. Allwood J, Erban A, de Koning S, Dunn W, Luedemann A, et al. (2009) Inter-laboratory reproducibility of fast gas chromatography-electron impact-time of flight mass spectrometry (GC-EI-TOF/MS) based plant metabolomics. *Metabolomics*: 479-496.
90. Kopka J, Schauer N, Krueger S, Birkemeyer C, Usadel B, et al. (2005) GMD@CSB.DB:the Golm Metabolome Database. *Bioinformatics*: 1635-1638.
91. Hummel J, Strehmel N, Selbig J, Walther D, Kopka J (2010) Decision tree supported substructure prediction of metabolites from GC-MS profiles. *Metabolomics*: 322-333.
92. Lommen A (2009) MetAlign: interface-driven, versatile metabolomics tool for hyphenated full-scan mass spectrometry data preprocessing. *Anal Chem* 81: 3079-3086.
93. Saeed AI, Sharov V, White J, Li J, Liang W, et al. (2003) TM4: a free, open-source system for microarray data management and analysis. *Biotechniques* 34: 374-378.